Food Hydrocolloids 144 (2023) 108934

Contents lists available at ScienceDirect

Food Hydrocolloids

journal homepage: www.elsevier.com/locate/foodhyd

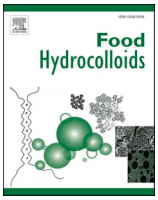

Biobased ternary films of thermoplastic starch, bacterial nanocellulose and gallic acid for active food packaging

Tânia Almeida [a], Anna Karamysheva [a], Bruno F.A. Valente [a], José M. Silva [a], Márcia Braz [b], Adelaide Almeida [b], Armando J.D. Silvestre [a], Carla Vilela [a,**], Carmen S.R. Freire [a,*]

[a] CICECO – Aveiro Institute of Materials, Department of Chemistry, University of Aveiro, 3810-193, Aveiro, Portugal
[b] CESAM & Department of Biology, University of Aveiro, 3810-193, Aveiro, Portugal

ARTICLE INFO

Keywords:
Thermoplastic starch
Bacterial nanocellulose
Gallic acid
Antioxidant and antibacterial activities
Oxygen barrier properties
Active food packaging

ABSTRACT

The use of active packaging technologies and biopolymeric materials are among the emerging trends for implementation of sustainability in the food packaging industry. Thus, herein, bioactive transparent nanocomposite films of thermoplastic starch (TPS) reinforced with bacterial nanocellulose (BNC) (1%, 5% and 10% w/w, relative to starch) and enriched with gallic acid (GA) (1 and 1.5% w/w, relative to starch) were prepared by the solvent casting method. The addition of BNC (≥5% w/w) and GA (1 and 1.5% w/w) enhanced both the mechanical properties (Young's Modulus: 1.2–2.0 GPa vs. 1.0 GPa for TPS; tensile strength: 23–39 MPa vs. 20 MPa for TPS) and the water resistance (moisture absorption and solubility in water) of the nanocomposites. All films are thermally stable up to 125 °C. It was also found that the addition of GA imparted the hydrocolloid TPS-BNC nanocomposites with UV-blocking properties and antioxidant activity (DPPH scavenging activity above 80%). In addition, the film with 10% w/w of BNC nanofibers and 1% w/w of GA had good oxygen barrier properties with a coefficient of permeability of 0.91 ± 0.12 cm^3 μm m^{-2} d^{-1} kPa^{-1} and antibacterial activity against the gram-positive *Staphylococcus aureus* (reduction of about 4.5 log_{10} colony forming units (CFU) mL^{-1} after 48 h). This is the first time that antibacterial activity is reported for TPS-BNC nanocomposites. The film with 10% w/w of BNC nanofibers and 1% w/w of GA was further demonstrated to have the ability of delaying the browning and weight loss of packaged fresh cut apple stored at +4 °C for 7 days. All these outcomes are of great relevance for the packaging sector, thus attesting the potential of the developed TPS-BNC-GA nanocomposites as sustainable and eco-friendly film materials for active food packaging.

1. Introduction

The importance of plastics for the global economy and our daily lives is unquestionable. Nevertheless, the environmental concerns raised by their massive use and, the finite availability of fossil resources used to produce conventional plastics (Rosenboom et al., 2022), altogether with the environmental awareness of consumers and the pressure of global environmental policies are driving the industrial transition towards more sustainable and environmentally friendly materials (Cavaliere et al., 2020). Food packaging, in particular, is one of the major generators of plastic waste and, consequently, the materials used in this sector are witnessing a great change (Guillard et al., 2018; Porta et al., 2022). In this context, biopolymers, owing to their biodegradability, renewability, and ability to meet most of the requirements of packaging materials (e.g., mechanical, barrier and optical properties), either used alone or blended with reinforcements and/or other additives, have been gaining relevance as green and viable alternatives to fossil-based plastics (Moustafa et al., 2019). In fact, the biopolymers' packaging market is expected to grow at a compound annual growth rate (CAGR) of 12.6% in the forecast period of 2021–2026 (Mordorintelligence, 2021), which evidences the increasing concern of this sector on the exploitation of biobased materials.

Among the multiple available biopolymers, starch is recognized as one of the most promising ones to be applied in the production of packaging materials since it is fully biodegradable, non-toxic, abundantly available, and it has a low cost and ability to be converted into a bioplastic material (Cheng et al., 2021; Jiang et al., 2020). Starch is a hydrocolloid polysaccharide produced by plants and algae, comprising

* Corresponding author.
** Corresponding author.
E-mail addresses: cvilela@ua.pt (C. Vilela), cfreire@ua.pt (C.S.R. Freire).

https://doi.org/10.1016/j.foodhyd.2023.108934
Received 8 December 2022; Received in revised form 27 May 2023; Accepted 30 May 2023
Available online 6 June 2023

long chains of glucose units linked together by α-1,4 and α-1,6 glycosidic bonds (Cheng et al., 2021; Compart et al., 2021). At the molecular level, starch is composed by two main macromolecular constituents, namely amylose and amylopectin (Cheng et al., 2021). Native starch can be converted into thermoplastic starch (TPS) by applying heat and shear force to the starch granules in the presence of adequate amounts of water and other plasticizers (e.g., glycerol, sorbitol, or polyethylene glycol) (Bodîrlău et al., 2014). The water and other plasticizers enhance the polymer flexibility and processability through disruption of the molecular interactions between the starch chains (Khan et al., 2017). Hence, with the possibility of using industrial thermal processing techniques (extrusion, injection moulding, *etc*.), similar to conventional thermoplastics, TPS is perceived as an attractive candidate to replace the traditional synthetic polymers (e.g., polyethylene, ethylene vinyl alcohol copolymer (EVOH)) used in food packaging (García-Guzmán et al., 2022; Lauer & Smith, 2020). However, TPS exhibits some weaknesses, namely poor mechanical properties (low tensile strength) and high sensitivity to moisture that hamper its broader application as a packaging material (Pérez-Pacheco et al., 2016). To overcome some of these limitations, the formulation of TPS-based composites reinforced with cellulosic fibres, whose similarity with the chemical structure of starch, foresees a good compatibility between both biopolymers (Montoya et al., 2014), has gained deal of great interest. Nanocelluloses forms, in particular, have demonstrated to be effective reinforcement agents in improving the mechanical properties of TPS-based films as demonstrated in works with cellulose nanofibers (CNFs) (Fazeli et al., 2018; Park et al., 2019), cellulose nanocrystals (CNCs) (González et al., 2020) or bacterial nanocellulose (BNC) (Martins et al., 2009; Osorio et al., 2014). Additionally, in some cases, the water resistance and thermal stability of TPS-based films were also found to be enhanced by the addition of nanocelluloses (Fazeli et al., 2018; Osorio et al., 2014).

Bacterial nanocellulose is a particularly fascinating hydrocolloid nanocellulose substrate produced extracellularly by several non-pathogenic bacteria, from which, the most used strains belong to the genus *Komagataeibacter* (formerly *Gluconoacetobacter*) (Torres et al., 2019). Besides its inherent biodegradability and renewable character, BNC also exhibits a set of other properties that turn it very appealing, namely the superior mechanical strength, high crystallinity, high thermal stability, and high purity (Cacicedo et al., 2016; Klemm et al., 2011). Another interesting feature of BNC is the fact that agro-industrial residues can be used, as fermentation medium, for its production (Costa et al., 2017; Gomes et al., 2013; Kumar et al., 2019), which, in one way, contributes to reduce the overall costs and, on the other, meets the principles of circular bioeconomy and sustainable development. Although the combination of TPS and BNC has already been investigated in several studies (Abral et al., 2021; Fabra et al., 2016; Grande et al., 2008; Martins et al., 2009; Montoya et al., 2014, 2019; Orts et al., 2005; Osorio et al., 2014; Santos & Spinacé, 2021; Wan et al., 2009; Wang et al., 2015), only some of them point out food packaging as a potential application (Abral et al., 2021; Fabra et al., 2016; Martins et al., 2009; Montoya et al., 2019; Osorio et al., 2014; Santos & Spinacé, 2021). The others are mainly focused on the method of production and characterization of the material, without targeting a specific application (Grande et al., 2008; Montoya et al., 2014; Orts et al., 2005; Wan et al., 2009; Wang et al., 2015). However, among the works directed to packaging, the research is mostly limited to the improvement of the mechanical behaviour, moisture sensitivity or barrier properties. But, in recent years, there were considerable advances in the packaging technology with the emergence of the concept of active packaging, *viz*. packages containing active compounds intended to extend or preserve products quality, safety, or shelf-life (Carvalho et al., 2021; Vilela et al., 2018). The food packaging sector has made great investment and progresses in this field (Vasile & Baican, 2021; Yildirim et al., 2018). Therefore, beyond the mechanical and barrier properties, other functionalities, such as antioxidant and antimicrobial activities or UV- barrier properties, are valued in the designof innovative packaging materials.

Additives, like natural phenolic compounds, have received special attention, since they are widely present in plants and are often described as having antioxidant, antimicrobial and UV-barrier properties (Martillanes et al., 2017). Among the multitude of natural phenolic compounds, gallic acid (3,4,5-trihydroxybenzoic acid, GA) is a low-cost compound, described as a powerful antioxidant with antimicrobial properties (Badhani et al., 2015), which is present, for example, in *Pinus pinaster* bark (Ferreira-Santos et al., 2019), *Suaeda glauca* Bge leaves (Wang et al., 2016), black tea (Souza et al., 2020) or in pineapple industry wastes (Sepúlveda et al., 2018), and thus, it is an interesting candidate to be explored as active agent. Indeed, in the field of food packaging, besides the incorporation in gelatin (Limpisophon & Schleining, 2017; Luo et al., 2021) and chitosan films (Zarandona et al., 2020), GA has already been loaded in starch films produced from potato by-products using the subcritical fluid technology, with the results showing that GA has provided those films with antioxidant properties (Zhao & Saldaña, 2019). Regarding BNC, it was also found that the incorporation of a GA-based ionic liquid into BNC membranes resulted in materials with antioxidant and anti-inflammatory activities, but in this case, for healthcare purposes (Morais et al., 2019).

Nevertheless, and to the best of our knowledge, the development of nanocomposite films composed of TPS, BNC and GA has never been studied. Therefore, it is a pertinent research topic to explore and investigate the gains of combining these two biopolymers with this phenolic acid in order to evaluate, not only the active properties of the resulting composite, but also whether some of the limitations of starch, as food packaging material, are surpassed.

Hence, the aim of this study was to develop TPS-based films reinforced with BNC nanofibers and loaded with GA to produce active TPS-BNC-GA nanocomposite films with antioxidant, antimicrobial and UV-barrier properties for potential application as sustainable active food packaging materials. A set of TPS-BNC-GA films, with different contents of BNC and gallic acid, was prepared and characterized in terms of structure, morphology, thermal stability, mechanical performance, water resistant properties (moisture absorption, solubility in water), optical properties, antioxidant activity, oxygen permeability (OP), antibacterial activity against the Gram-positive *Staphylococcus aureus* and applicability in preserving fresh-cut apple stored at +4°C.

2. Materials and methods

2.1. Chemicals, materials and microorganisms

Citric acid (≥99.5%), disodium hydrogen phosphate (≥99.0%), glucose (≥99.5%), glycerol (≥99.5%), potassium chloride (≥99.0%), potassium phosphate monobasic (≥99.0%), sodium chloride (≥99.0%), 2,2-diphenyl-1-picrylhydrazyl (DPPH) and potato starch (20% amylose and 80% amylopectin) (Zhao et al., 2019) were purchased from Sigma-Aldrich (Lisbon, Portugal). Tryptic Soy Agar (TSA) and Tryptic Soy Broth (TSB) were supplied by Liofilchem (Roseto degli Abruzzi TE, Italy). Peptone and yeast extract were acquired from Himedia Laboratories GmbH (Einhausen, Germany). All other chemicals were of laboratory grade.

BNC was produced in our laboratory using the acetic acid bacteria *G. sacchari* grown in Hestrin-Schramm (HS) culture medium (20 g L^{-1} glucose, 5 g L^{-1} peptone, 5 g L^{-1} yeast extract, 2.7 g L^{-1} disodium hydrogen phosphate, 1.15 g L^{-1} citric acid, pH 5) under static culture conditions at 28 °C for 4–5 days (Trovatti et al., 2011). The resulting BNC membranes were recovered and purified following a previously described methodology (Almeida et al., 2022). Subsequently, the purified BNC membranes were disintegrated with a MiniBatch D-9 homogenizer (MICCRA GmbH, Heitersheim, Germany) during 25 min at 16000 rpm to obtain the BNC nanofibers.

Staphylococcus aureus DSM 25693 bacterium, a methicillin resistant (MRSA) strain was provided by DSMZ – Deutsche Sammlung von Mikroorganismen und Zellkulturen GmbH (German Collection of Microorganisms and Cell Cultures).

2.2. Films preparation

Potato starch powder (2% w/v) was dispersed in distilled water and the obtained suspension was then heated in an oil bath at 95 °C for 30 min with stirring (500 rpm) to promote the gelatinization of starch. After this step, the starch solution was cool down to ca. 40–50 °C and then glycerol (20% w/w, on starch dry basis) was added, and the solution stirred for another 1 h. The TPS-BNC films were prepared by adding different contents of disintegrated BNC (1, 5 and 10% w/w, on starch dry basis) to the starch solution. To prepare the TPS-BNC-GA films, two different GA concentrations (1 and 1.5% w/w, on starch dry basis) were added simultaneously with BNC. A control film consisting of only of TPS was also prepared. All formulations were casted on polystyrene moulds and placed in an air-ventilated oven at 35 °C during at least 20 h for solvent evaporation. After drying, films were carefully peeled off from the mould and stored at room temperature and 50 ± 5% relative humidity (RH) and protected from light. The identification and composition of all the prepared films are presented in Table 1.

2.3. Films characterization

All TPS-based films were characterized regarding their thickness, morphology, structure, thermal stability, water resistant properties (moisture absorption and solubility in water), optical properties and antioxidant activity (DPPH free radical scavenging). Based on the results of these characterizations, the composite film TPS-BNC10-GA1 was selected and further characterized in terms of oxygen permeability, antibacterial activity against *S. aureus* and applicability in preserving fresh-cut apple stored at 4 °C.

2.3.1. Thickness

Films thickness was measured using a hand-held digital micrometer Mitutoyo (Mitutoyo Corporation, Japan) with an accuracy of 1 μm. Measurements were taken at five different randomly locations and the mean value and standard deviation were calculated.

2.3.2. Morphology

The surface and cross-section morphology of the films was analyzed by scanning electron microscopy (SEM). Micrographs were obtained using a high voltage microscope (HR-FESEM SU 70 Hitachi, Tokyo, Japan) operated at a low voltage of 1.5 kV to minimize the risk of damaging the surface of the film. Prior to image acquisition, samples were placed on an aluminium support and coated with a carbon film. The cross-sections of the films were obtained by breaking the films after immersion in liquid nitrogen.

2.3.3. Structure

2.3.3.1. Infrared spectroscopy. The structure of the films was studied by Attenuated Total Reflection – Fourier Transformed Infrared (ATR-FTIR) spectroscopy using a Perkin-Elmer FT-IR system Spectrum BX-spectrophotometer (Perkin-Elmer Inc., Waltham, Massachusetts, USA) equipped with a single horizontal Golden Gate ATR cell. The ATR-FTIR spectra were acquired over the wavenumber range of 600–4000 cm^{-1} with a resolution of 4 cm^{-1} in a total of 32 scans.

2.3.3.2. X-ray diffraction (XRD). The XRD patterns of all nanocomposite films were performed on an Empyrean X-ray diffractometer (Malvern Panalytical, Malvern, United Kindgom) operated at a voltage of 45 kV and 40 mA using CuK radiation (λ= 1.541 Å) in an angular range of 5–50° (2θ) and at a scanning speed of 1° min^{-1}. The XRD patterns were acquired in reflection mode with the films placed on a Si wafer with negligible background signal.

2.3.4. Thermal stability

Thermogravimetric analysis (TGA) was conducted with a Hitachi STA300 analyzer (Hitachi, Tokyo, Japan) equipped with a platinum cell. The samples were heated from room temperature to 800 °C at a constant rate of 10 °C min^{-1} under a nitrogen atmosphere.

2.3.5. Mechanical performance

The mechanical performance of the films was studied by uniaxial tensile tests using an Instron 5966 testing machine (Instron, Norwood, Massachusetts, USA) in the traction mode with a 500 N static load cell at a cross-head speed of 10 mm min^{-1} and with a gauge length of 30 mm. Before testing, rectangular strips of each film (50 × 10 mm^2) were equilibrated at room temperature and 50 ± 5% RH for 24 h. Stress (MPa) and strain (%) curves were plotted and the tensile strength, the Young's Modulus and the elongation at break were calculated using the Instron BlueHill 3 software. Six replicates were analyzed for each film.

2.3.6. Water resistance properties

2.3.6.1. Moisture absorption. The moisture absorption capacity was evaluated by placing the dry films specimens (20 × 20 mm^2) in a conditioned container at about 75% RH (with a saturated sodium chloride aqueous solution) (Greenspan, 1977) and at room temperature for 2 h, 6 h, 24 h and 72 h. At each time point, the specimens were weighted (W_w), and the moisture absorption was calculated according to the equation:

$$Moisture\ absorption\ (\%) = \frac{W_w - W_0}{W_0} \times 100$$

where W_0 is the initial weight of the dry film. Temperature and environment air moisture inside the container were monitored using a digital temperature and humidity meter.

2.3.6.2. Solubility in water. The water solubility of the films was assessed following a previous described method (Núñez-Flores et al., 2012). Briefly, film samples (20 × 20 mm^2) were dried (60 °C, 4 h), weighed and placed in flasks with 25 mL of distilled water and then let to stand at room temperature for 24 h. After that, the films were recovered

Table 1
Identification, composition and thickness values (± standard deviation) of the prepared films.

Film	Starch (% w/v)	Glycerol (%)[a]	BNC (%)[a]	Gallic acid (%)[a]	Thickness (μm)
TPS	2	20	–	–	28 ± 2
TPS-BNC1	2	20	1	–	33 ± 3
TPS-BNC1-GA1	2	20	1	1	33 ± 3
TPS-BNC1-GA1.5	2	20	1	1.5	33 ± 2
TPS-BNC5	2	20	5	–	33 ± 2
TPS-BNC5-GA1	2	20	5	1	34 ± 2
TPS-BNC5-GA1.5	2	20	5	1.5	36 ± 2
TPS-BNC10	2	20	10	–	35 ± 2
TPS-BNC10-GA1	2	20	10	1	35 ± 1
TPS-BNC10-GA1.5	2	20	10	1.5	36 ± 1

[a] w/w relative to starch.

in a filter paper and dried at 105 °C for 24 h. The solubility of each film was calculated by the equation:

$$Solubility\ in\ water\ (\%) = \frac{W_0 - W_f}{W_0} \times 100$$

where W_0 is the initial weight of the films and W_f is the weight of the undissolved dried film fraction. Measurements were carried out in five replicates.

2.3.7. Optical properties

The transmittance spectra of the films were acquired with an Ultraviolet–visible (UV–vis) Multiskan Go spectrophotometer (Thermo Fischer Scientific, Waltham, Massachusetts, USA). The spectra of the films (40 × 10 mm^2) were recorded at room temperature in the range of 200–800 nm. Additionally, the opacity of films was determined at 600 nm by the following equation (Wang et al., 2018):

$$Opacity = \frac{A_{600}}{x}$$

where A_{600} is the absorbance at 600 nm and x is the mean thickness (mm) of the film. Measurements were performed in triplicate and the mean value with the respective standard deviation were calculated.

2.3.8. Antioxidant activity

The antioxidant activity of the films loaded with GA was evaluated by the DPPH free radical scavenging method as described elsewhere (Moreirinha et al., 2020), with minor modifications. Films of TPS and TPS-BNC without GA were also analyzed for comparison purposes. Briefly, a film sample (10 × 10 mm^2) was added to 4 mL of an ethanol/water (1:1) solution and then, 250 μL of 1 mM DPPH in ethanol was added (0.06 mM final concentration). The mixture was incubated at room temperature, in the dark, with slight agitation (80 rpm) during 2 h. At the end of this incubation period, the absorbance was measured at 517 nm in a Thermo Scientific Multiskan™ FC microplate reader (Thermo Fischer Scientific, Waltham, Massachusetts, USA). The DPPH scavenging activity was calculated using the following equation:

$$DPPH\ scavenging\ activity\ (\%) = \frac{(A_{DPPH} - A_{sample})}{A_{DPPH}} \times 100$$

where A_{sample} is the absorbance of the ethanolic solution containing the film sample and A_{DPPH} is the absorbance of the control (viz. ethanol/water solution with DPPH but without film sample). Samples were analyzed in triplicate.

2.3.9. Oxygen permeability

The oxygen permeability of the films (TPS, TPS-BNC10 and TPS-BNC10-GA1) was determined in accordance with the ISO-15105-2:2003, at 23 °C and 50% RH using the Labthink Perme OX2/230 equipment (Labthink International, Inc, Medford, Massachusetts, USA). Film samples were enveloped in an aluminum foil mask, leaving an exposed tested area of 5.31 cm^2. Prior to analysis, all samples were conditioning at 23 °C and 50% RH for 24 h. The oxygen concentration in the test gas was 99.96% and the carrier gas was 99.99% nitrogen. Measurements were performed, in duplicate, under atmospheric pressure.

2.3.10. In vitro antibacterial activity

Film samples (TPS, TPS-BNC10 and TPS-BNC-GA1) were tested against *S. aureus* DSM 25693 MRSA. Prior to the test, film samples (small pieces of 1 cm^2) were UV-sterilized during 20 min on each side. The bacteria were grown on solid medium (TSA) at 37 °C during 24 h and posteriorly kept at 4 °C. Before each assay, one isolated colony was inoculated in 30 mL of TSB medium and grown aerobically at 25 °C overnight, for 18–24 h, under stirring (120 rpm). An aliquot of this culture (300 μL) was transferred into a new fresh TSB liquid medium and grew under the same growth conditions until stationary growth phase was achieved (≈ 10^9 colony forming units per mL (CFU mL^{-1})). Then, the bacterial culture was diluted in phosphate buffer saline (PBS) (137 $mmol^{-1}$ NaCl, 2.7 $mmol^{-1}$ KCl, 8.1 $mmol^{-1}$ $Na_2HPO_4{\cdot}2H_2O$, 1.76 $mmol^{-1}$ KH_2PO_4, pH 7.4) to obtain a bacterial suspension with 10^5 CFU mL^{-1} of concentration and further incubated with film samples (3 cm^2 (3 pieces of 1 cm^2) mL^{-1}) at 25 °C during 48 h. Aliquots of 100 μL were taken at 0, 24 and 48 h of incubation and serially diluted in PBS. Then, two drops per dilution (10 μL each) were plated onto TSA medium, by the drop plate method. After the drops dried, the Petri plates were inverted and incubated at 37 °C for 18−24 h to determine the concentration of bacteria (CFU mL^{-1}) by colonies counting on the most appropriate dilution. A negative control consisting in *S. aureus* bacterial suspension (10^5 CFU mL^{-1}) without film sample was also included in the test. Three independent assays with two replicates each were performed and the average of the results was calculated.

2.3.11. Evaluation of films performance on preserving fresh-cut apple

2.3.11.1. Experimental set-up. Apples (*Malus domestica* Borkh cv. Gala) were purchased at Aveiro (Portugal) at a local market. Fruits, with a diameter between 65 and 70 mm, were chosen accordingly to color uniformity and absence of physical defects. The selected fruits were washed with distilled water, peeled, and cut in half using a stainless-steel knife. Afterwards, each fruit half was cut into roughly cubed shaped pieces (~2.0 × 2.0 × 2.0 cm^3), and immediately immersed in a sodium hypochlorite (NaClO) solution at 100 ppm for 10 min for disinfection, followed by immersion in distilled water for 10 min to remove the NaClO. Then, the apple samples were dried with absorbent paper and placed in aluminum trays coated on the bottom and covered on the top with the prepared films (TPS, TPS-BNC10, TPS-BNC10-GA1), in sets of 3 apple cubes per tray. After sealing, each container was stored in a refrigerator at +4 ± 1 °C for 7 days. For comparison purposes, samples with no film, and with commercial low-density polyethylene (LDPE) film were also prepared. Fresh apple samples were analyzed on the 3rd and 7th day of storage regarding their physical appearance, browning index (BI), weight loss and pH.

2.3.11.2. Physical appearance and BI. The physical appearance of fresh apple samples was recorded and the color parameters, expressed in the CIELab scale (L*, a* and b*), were analyzed using a Konica Minolta CM-2300d portable sphere type spectrophotometer with horizontal alignment (Konica Minolta Sensing Europe B.V., UK) and the Spectra Magic™ NX software, after prior calibration with a white calibration plate. The color measurements were acquired at five randomly selected sites of the fruit cubes and performed in triplicate for each aluminum tray. The BI was calculated according to the following equation (Jiang et al., 2022):

$$BI = \frac{[100(X - 0.31)]}{0.172}$$

where $X = \frac{(a^* + 1.75L^*)}{(5.64L^* + a^* - 3.012b^*)}$.

2.3.11.3. Weight loss. The weight loss of the fresh-cut apple samples was determined from the difference between the initial weight (W_i) of each fruit cube and its respective weight at the day n (W_n) of the storage time as shown by the following equation:

$$Weight\ loss\ (\%) = \frac{W_i - W_n}{W_i} \times 100$$

These measurements were performed in triplicate.

2.3.11.4. pH. The pH of the fresh-cut apple samples was measured according to the AOAC method. Briefly, 10 g of fruit were triturated with a hand blender with 100 mL of distilled water, and the pH of the solution measured using a digital benchtop pH meter. Five measurements were carried out for each sample.

2.4. Statistical analysis

All data are expressed as mean ± standard deviation. Statistical significance was assessed applying a one-way analysis of variance (ANOVA) followed by Tukey's test (GraphPad Prism software 8.0.2). Statistical significance was established at $p < 0.05$.

3. Results and discussion

Novel nanocomposite TPS films, reinforced with BNC nanofibers and loaded with gallic acid, GA, were prepared through the solvent casting method (Fig. 1). Different contents of BNC nanofibers (1, 5 and 10% w/w, relative to starch) and GA (1.0 and 1.5% w/w, relative to starch) were

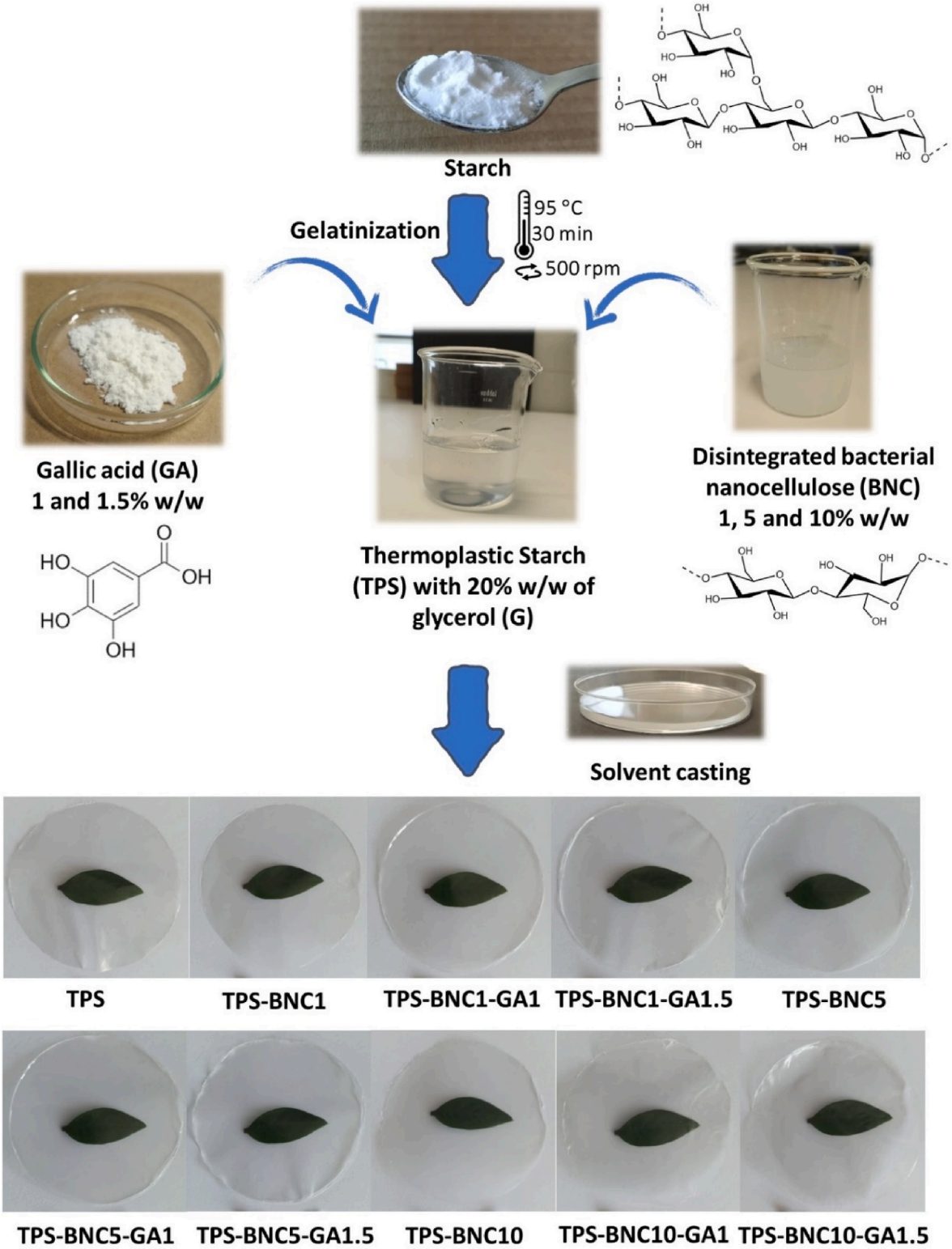

Fig. 1. Scheme showing the preparation of the TPS-BC-GA nanocomposite films by solvent casting, and the corresponding digital photographs with films placed on the top of a plant leaf to evidence their transparency.

investigated (Table 1) to evaluate their influence on the properties of the nanocomposite films and, thus, select the most promising formulations for potential application as active packaging materials.

The obtained TPS-based nanocomposite films were then characterized in terms of their thickness, structure, morphology, thermal stability, mechanical behaviour and water resistance (moisture absorption and the solubility in water). The optical properties and the antioxidant activity (DPPH free radical scavenging) of all nanocomposites were also evaluated. Based on the obtained results, the film containing 10% w/w of BNC nanofibers and 1% w/w of GA, was selected to further analyse the oxygen permeability, the antibacterial activity against *S. aureus* and applicability on preserving fresh-cut apple stored at +4 °C.

As depicted in Fig. 1, all the resulting films are macroscopically homogeneous and exhibit a transparent appearance, that slightly decreased with the increasing content of BNC. Regarding the thickness of films, it increased from ca. 28 μm in the TPS film to values between 33 and 36 μm in nanocomposite films containing BNC and GA (Table 1).

3.1. Structure

3.1.1. ATR-FTIR spectroscopy

The structure of the TPS, TPS-BNC and TPS-BNC-GA films, as well as, of their precursors (starch, BNC, glycerol and GA) was analyzed by ATR-FTIR spectroscopy. As presented in Fig. 2, the spectra of the nanocomposite films are similar to those of native starch and TPS film, with a typical spectrum of polysaccharides, showing the characteristic broad absorption bands at around 3300 cm^{-1} credited to vibrations of O–H groups associated with intra and intermolecular hydrogen bonds in BNC and of starch, water and glycerol in TPS (Nguyen Vu & Lumdubwong, 2016; Santos & Spinacé, 2021). The bands at around 2900 cm^{-1}, 1150 cm^{-1} and 1000-1080 cm^{-1} are attributed to the stretching of the C–H, C–O–C and C–O functional groups, respectively (Abdullah et al., 2018). Albeit the similarity between spectra, the single peak that appears in native starch at 996 cm^{-1}, related to the C–O stretching, is transformed into two peaks at around 996 and 1010 cm^{-1} in TPS and in the ensuing nanocomposite films. This may be associated with the plasticization effect of glycerol due to the weakening of intra and inter-molecular hydrogen bonds between the starch chains (Nguyen Vu & Lumdubwong, 2016). An absorption band is also observed at around 1650 cm^{-1}, which is typically assigned with the deformation vibration of the adsorbed water molecules to starch (Nguyen Vu & Lumdubwong, 2016; Zhao & Saldaña, 2019). Moreover, the absorption band at around 1415 cm^{-1} corresponds to the presence of C–H symmetrical scissoring of $–CH_2OH$ moieties of starch and cellulose chains (Abdullah et al., 2018). The similarity of the spectra of TPS and of the nanocomposites, not showing new peaks or significant shifts in peaks position, is also indicative that there are no substantial changes in the structure of the starch matrix and confirming the good compatibility between the matrix and the remaining components of the nanocomposites. It should also be noted that some absorption bands of common functional groups, are probably overlapped, given the analogous polysaccharidic structure of BNC and starch. On the other hand, the low loadings of the additives (glycerol and GA) in relation to starch, particularly of GA, may also explain the absence of the typical bands associated with these compounds.

3.1.2. X-ray diffraction

To complement the structural analysis of the ensuing nanocomposite films and infer about their crystalline/amorphous nature, XRD analysis was performed. The diffraction patterns depicted in Fig. 3 show that the

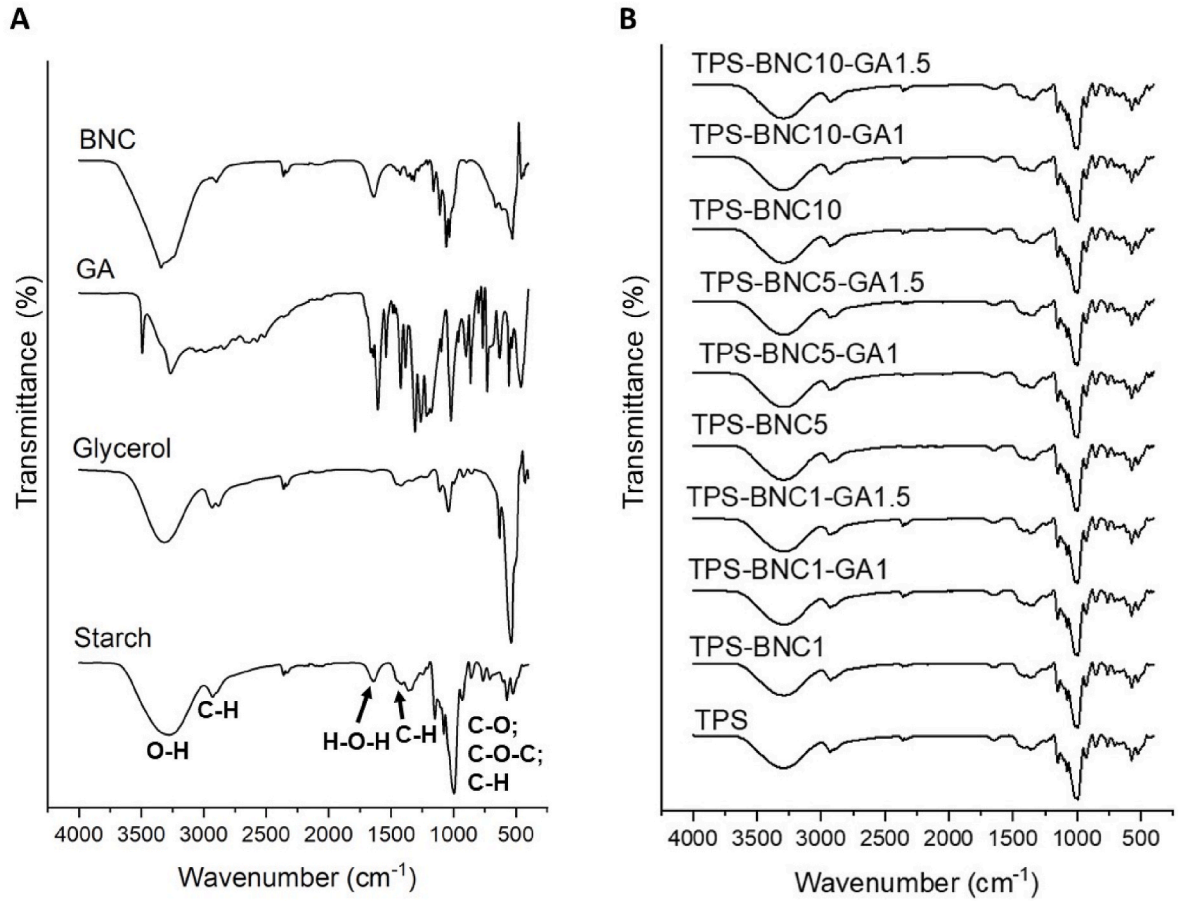

Fig. 2. ATR-FTIR spectra of (A) starch, glycerol, GA and BNC and of (B) TPS film and the TPS-based nanocomposite films with different contents of BNC and GA.

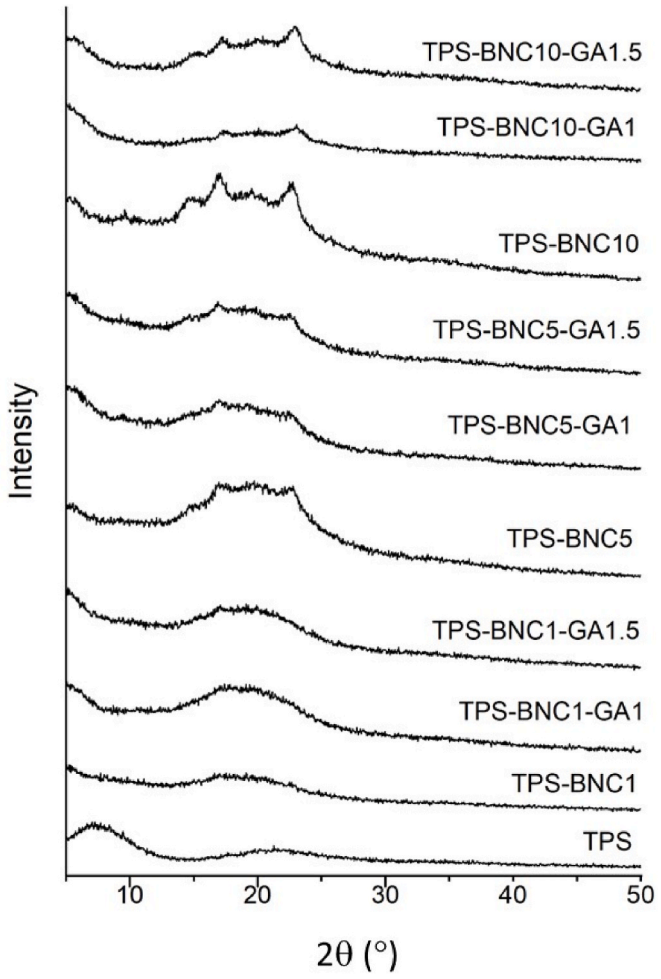

Fig. 3. X-ray diffractograms of TPS film and the TPS-based nanocomposite films with different contents of BNC and GA.

neat TPS film is essentially amorphous in nature, with a low intensity diffraction peak at about 2θ 7.4° representative of the V-type crystalline structure, which is indicative of some retrogradation of the gelatinized starch that may have occurred during drying (Wongprayoon et al., 2018). In the nanocomposites with 1% w/w of BNC nanofibers (TPS-BNC1), the diffraction pattern is still very characteristic of an amorphous material. With the increasing content in BNC nanofibers, the peaks at 2θ 17.0° and 22.5° become more pronounced. The peak at 2θ 17.0° could be associated with the starch B-crystalline structure, whereas the peak at 2θ 22.5° is attributed to the semi-crystalline structure of the BNC nanofibers (typical of type I cellulose). These results suggest, on the one hand, that the BNC nanofibers favor the retrogradation of starch, agreeing with results obtained by other authors (Martins et al., 2009) and, on the other, that the reinforcement boosted the crystallinity of the nanocomposite films. With the addition of GA, the crystallinity of nanocomposites slightly decreased, namely the intensity of the peak at 2θ 17.0°, suggesting that this compound may be delaying or preventing the re-crystallization of starch as previously reported for potato starch films loaded with GA, and that may be explained by the establishment of intermolecular H-bonding between the –OH groups of starch and GA (Zhao & Saldaña, 2019). A similar effect was also observed in potato starch-chitosan blend films containing ferulic acid (Mathew & Abraham, 2008) or in cassava starch films loaded with *yerba mate* extract (Jaramillo et al., 2016).

3.2. Morphology

The surface and cross-section morphology of all the obtained nanocomposite films was studied by SEM and the micrographs are compiled in Fig. 4. From the surface images, it is visible that the pure TPS film has a fairly smooth surface as previously observed by other authors (Chen et al., 2021). On the other hand, in the nanocomposite films, the addition of BNC nanofibers led to a slight increase in surface roughness, that it is intensified with the rise of the BNC content (Fig. 4). But, a quite good dispersion of BNC nanofibers was achieved in all nanocomposites with no visible pores or cracks on the surface of the films, being evident the embedment of the nanofibers into the TPS matrix. The micrographs also reveal that no evident differences were observed in the films containing GA, demonstrating that there were no agglomerates of GA formed during solvent evaporation. This is similar to what was previously reported for TPS films loaded with GA (Zhao & Saldaña, 2019). Analogous results were revealed by the cross-section images with an increasing rough morphology with the augment of the amount of BNC, but a general good dispersion and embedment of the BNC into the TPS matrix even for higher BNC contents. The formation of GA agglomerates is also not perceived in the cross-section micrographs. These observations confirmed the good compatibility and miscibility of the individual components of the nanocomposites, thus corroborating the visual aspect of the films._c

3.3. Thermal stability

The thermal behaviour of the prepared nanocomposite films was investigated by TGA, aiming at determining their thermal stability and degradation profile. The obtained TGA curves and their first derivative (DTG) are depicted in Fig. 5. All the ensuing films had a quite similar thermal behaviour displaying three distinct stages of weight loss. The first stage (<120 °C) with a small weight loss is associated with the volatilization of water molecules from the nanocomposites. The second one (125–240 °C) is attributed to the decomposition of glycerol, concurring with results obtained by other authors for starch-based films plasticized with glycerol (Menzel et al., 2019; Rodrigues et al., 2021). Moreover, the degradation of GA may also occur in this region at about 224 °C (Chen et al., 2020). The third step, which is the one with the highest weight loss, has maximum decomposition temperatures of about 300–310 °C (TPS: 306 °C; TPS-BNC1: 306 °C; TPS-BNC1-GA1: 306 °C; TPS-BNC1-GA1.5: 300 °C; TPS-BNC5: 309 °C; TPS-BNC5-GA1: 308 °C; TPS-BNC5-GA1.5: 309 °C; TPS-BNC10: 310 °C; TPS-BNC10-GA1: 306 °C; TPS-BNC10-GA1.5: 308 °C), that correspond to the extensive degradation of starch (the main component of the films), but also of BNC (Abral et al., 2021; Nunes et al., 2021). Although there are some variations in the values, the results suggest that these contents of BNC and GA do not significantly influence the maximum decomposition temperature of the nanocomposites. These results are in line with those of the XRD analysis in which only slight changes were observed in the crystallinity of the nanocomposites compared with TPS.

Finally, above 400 °C, the carbonization of residues of the starch-based films and formation of carbonaceous char takes place (Nunes et al., 2021), resulting in a final residue varying between 16 and 19%. In conclusion, the results indicate that all the developed nanocomposite films are stable up to 125 °C, which is still above of either the pasteurization (<100 °C) or the steam sterilization (110–121 °C) temperatures, that are common heat treatments applied by some industries to eliminate pathogenic microorganisms from packaged products (Chiozzi et al., 2022; Jildeh et al., 2021).

3.4. Mechanical performance

The poor mechanical properties of starch-based films are one of the limitations that hampers their broad application in packaging (Onyeaka et al., 2022). In order to verify the effect of the addition of BNC and GA

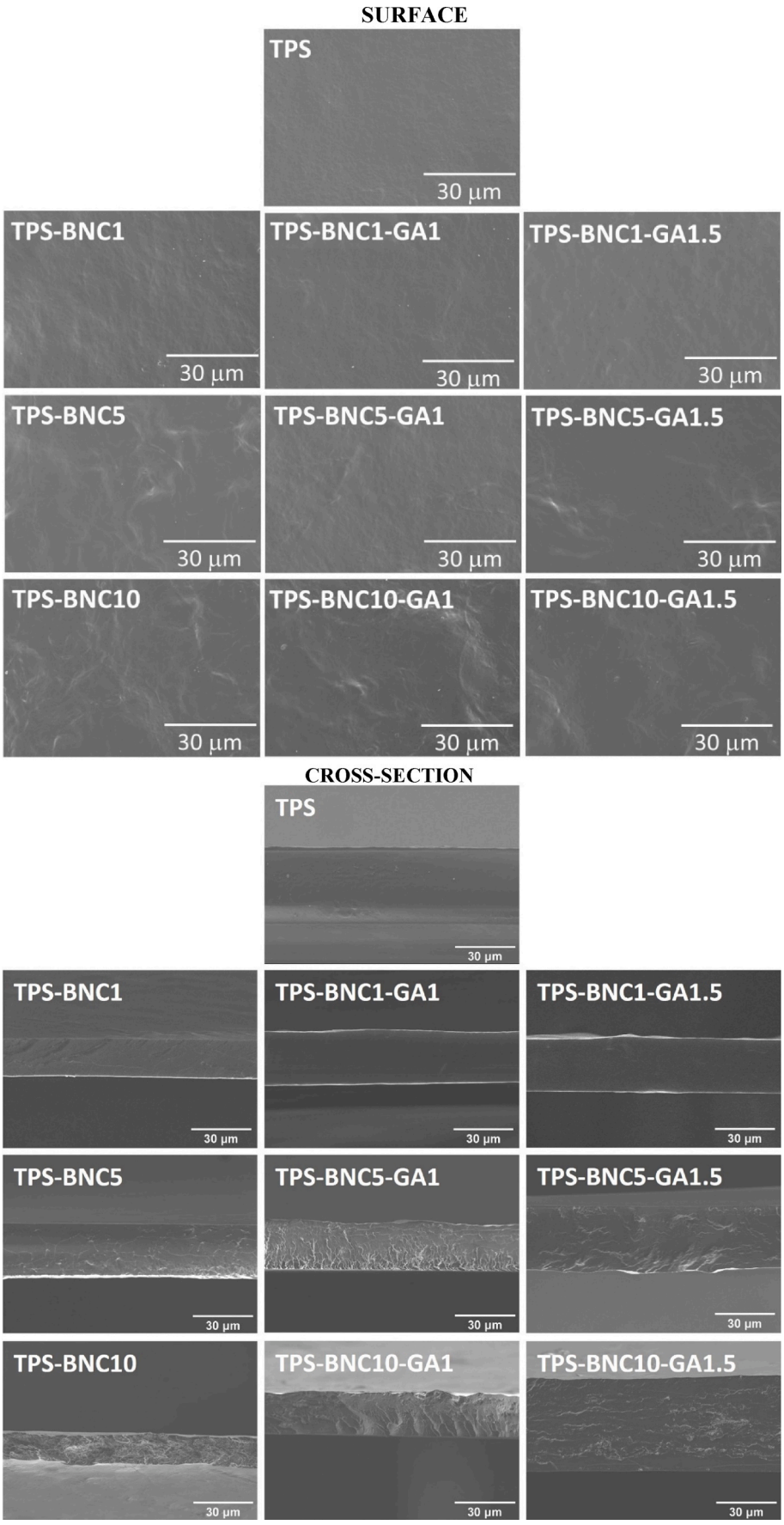

Fig. 4. SEM micrographs of the surface and cross-section of the TPS film and TPS-based nanocomposite films.

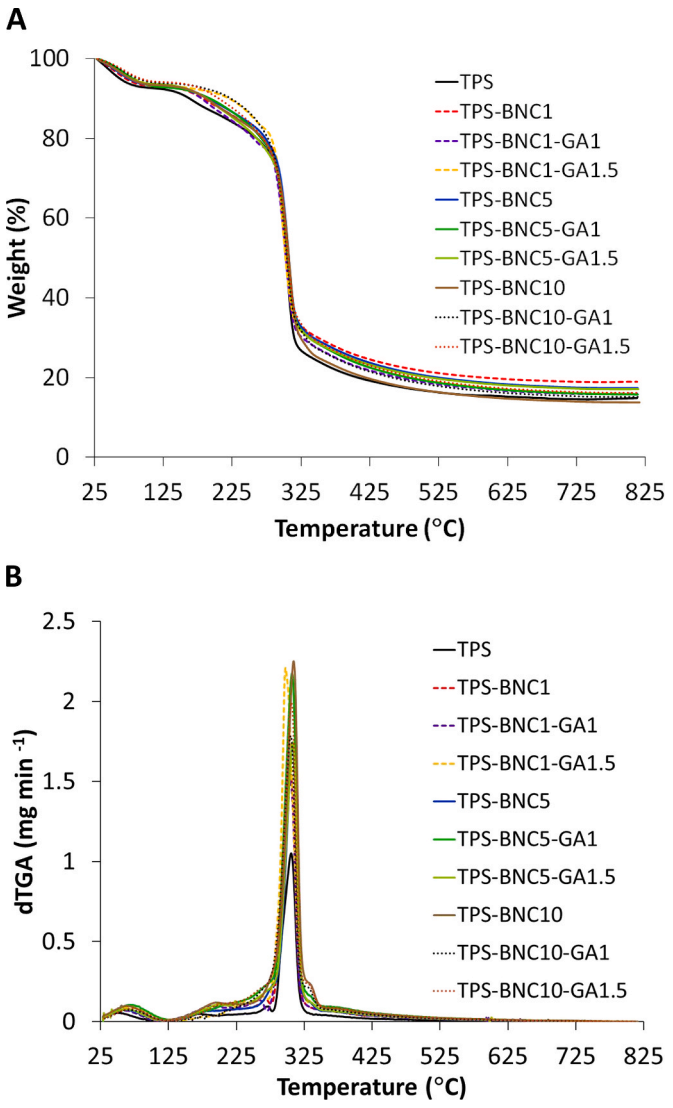

Fig. 5. (A) Thermogravimetric curves and (B) the respective derivatives of the TPS film and the TPS-based nanocomposite films with different contents of BNC and GA, under inert (N_2) atmosphere.

on the mechanical performance of the TPS films, their mechanical properties were evaluated by tensile tests.

The results of the tensile tests (Fig. 6A–C) confirmed that, as expected, the incorporation of BNC nanofibers into the TPS matrix resulted in more resistant films, with a clear increase of the Young's modulus (YM) and tensile strength (TS) with the rising in the content of BNC fibers. These results, on the one hand, reflect the compatibility between the plasticized starch matrix and BNC, anticipated by the above-mentioned structural similarity of the two hydrocolloid biopolymers and further evidenced in the SEM micrographs, that results in a better interfacial interaction and strong hydrogen bonding between them (Karimi et al., 2014). But, above all, the results highlight the character of BNC nanofibers as reinforcement agent of TPS, as intended. In fact, the reinforcement of TPS matrix with BNC nanofibers has been previously described (Hafizulhaq et al., 2018; Martins et al., 2009).

Although the reinforcement with BNC seems to be the main factor that is contributing to the strengthening of the nanocomposites, the incorporation of GA has also resulted in a slight increase in both YM and TS, especially in the nanocomposites comprising 5 and 10% w/w of BNC nanofibers, probably because of the formation of intermolecular hydrogen bonds between the –OH groups of GA and BNC and starch, that will contribute to a more stable and compact network (Mangmee & Homthawornchoo, 2016; Zhao & Saldaña, 2019). Specifically, the YM values of the nanocomposite films vary between 1.2 and 2.0 GPa (vs. 1.0 GPa for TPS) and the TS between 23 and 39 MPa (vs. 20 MPa for TPS), being the film with 10% w/w of BNC and 1.5% w/w of GA (TPS-BNC10-GA1.5), the nanocomposite that exhibits the highest values. The incorporation of phenolic compounds like GA (Rachtanapun & Tongdeesoontorn, 2009), water-soluble phenolic compounds extracted from rice straw waste (Menzel et al., 2020), and green tea extract (Mangmee & Homthawornchoo, 2016) in starch-based films has also demonstrated to result in more resistant films in a mechanical point of view.

Notably, the values of YM and TS, here obtained, are also in the range of those reported for synthetic polymers commonly used in flexible packaging, like EVOH (YM: 2.1–2.6 GPa; TS: 59–77 MPa) or LDPE (YM: 0.2–0.5 GPa; TS: 8–31 MPa) (Luzi et al., 2019; Mangaraj, Goswami, & Mahajan, 2009). Not surprisingly, this increase in strength, was accompanied by a significant reduction in the elongation at break for the nanocomposites with BNC and with BNC and GA (values in the range of 3.4–4.1%) when compared with pure TPS films (6.8%). However, for this parameter no significant variations between nanocomposites were perceived, regardless of the BNC and GA contents. In literature, the effect of GA on the elongation of starch-based films differs. While Zhao and Saldaña (2019) reported an increase in the elongation at break of starch-based films loaded with GA up to 0.2 g of GA/g of potato cull starch, Rachtanapun and Tongdeesoontorn (2009) described the opposite effect in rice flour/cassava starch film blends incorporating 0.04 g of GA/g rice/flour/cassava starch, where the elongation at break decreased from 20% (film without GA) to 14% (film with GA), similarly to what was observed here. This may be explained by the formation of the aforementioned intermolecular interaction between GA and starch, that will hinder the intramolecular mobility of starch chains, thus resulting in more rigid films (Menzel, 2020). The effect of cellulosic fibers on the reduction of the elongation of TPS films is also well known. Indeed, similar results were obtained for films based on TPS reinforced with cellulosic fibers, namely, TPS films with 10% microfibrillated cellulose showing an elongation at break of 2.5% (Nordin et al., 2018) or films of modified starch microparticles with TPS and with Microcell (micronized cellulose) recording a value of 3.7% (Bodîrlău et al., 2014). However, and albeit the reduction in the elongation at break of the TPS-BNC-GA films, it should be noted that, from a mechanical point of view, these nanocomposite films, regardless of the BNC and GA content, remain flexible enough to be handled, as illustrated in Fig. 6D.

3.5. Water resistance properties

3.5.1. Moisture absorption

Due to the hygroscopic nature of starch, another challenge for its application as a packaging material is to improve its resistance to ambient humidity in order to preserve its physical and barrier properties. In this sense, the effect of the addition of BNC nanofibers and GA on the ambient moisture absorption from the developed films was investigated.

The results (Fig. 7A) show that, although all films absorbed moisture over time, the addition of the BNC nanofibers and GA had a positive effect on this property. For the same time point, as the BNC content increases, a clear trend of reduction in the moisture absorption by the nanocomposites was observed. At 72 h, comparatively with neat TPS, films containing 10% w/w of BNC without or with GA (1 and 1.5% w/w) have effectively absorbed significantly less ($p < 0.05$) moisture from the environment. Specifically, whereas, in the neat TPS film the moisture absorption reached 8.9 ± 1.5%, in the nanocomposite films, this value is reduced to values between ca. 4.9 ± 0.6% for TPS-BNC10, 2.9 ± 0.5% for TPS-BNC10-GA1 and 3.1 ± 0.6% for TPS-BNC10-GA1.5, suggesting that they have higher resistance to ambient moisture, similarly to what was achieved by other authors for TPS films reinforced with cellulosic fibers (Bodîrlău et al., 2014; Hafizulhaq et al., 2018) or loaded with

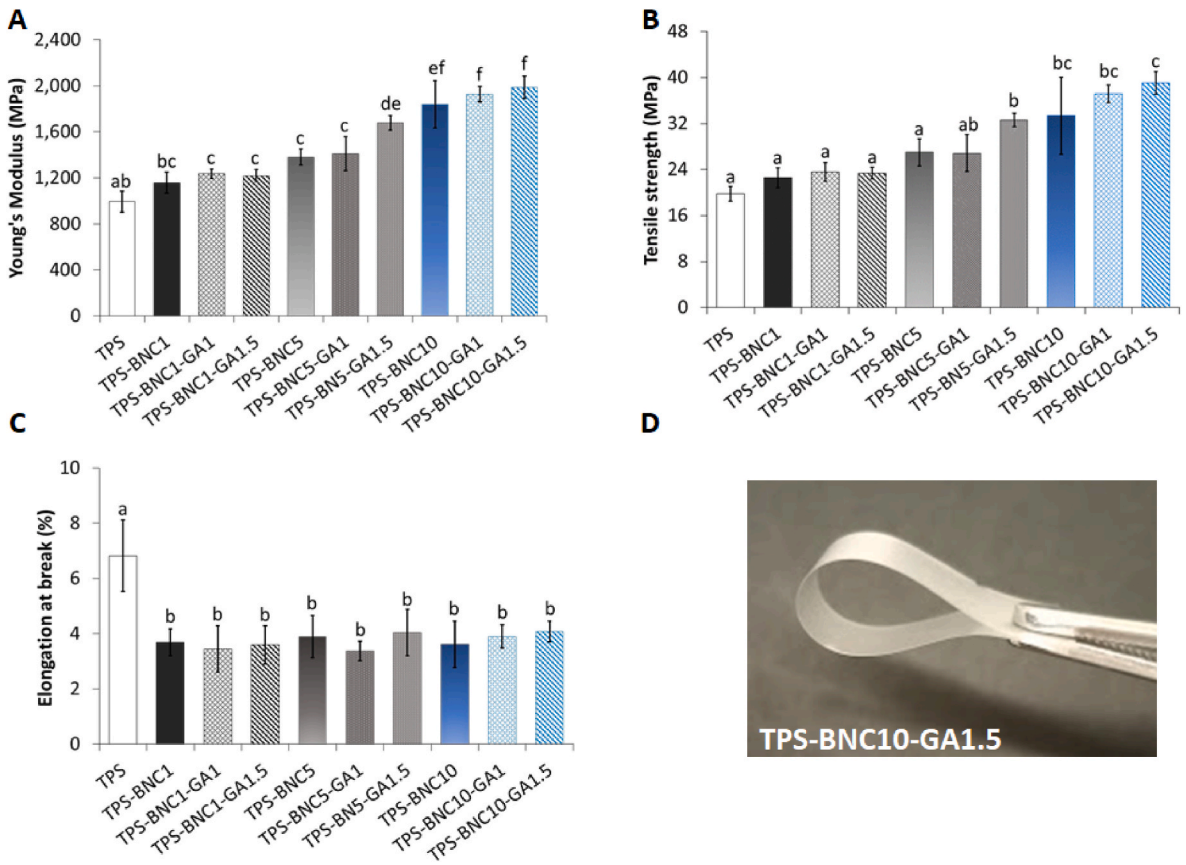

Fig. 6. (A–C) Mechanical properties (Young's modulus, tensile strength and elongation at break) of the TPS film and of the TPS-based nanocomposite films with different contents of BNC and GA. The values are the mean of five replicates and the error bars correspond to standard deviations. Means with different letters indicate a significant difference ($p < 0.05$); (D) photograph of the flexible TPS-BNC10-GA1.5 nanocomposite film.

yerba mate extract (Jaramillo et al., 2016). This reduction in moisture absorption by the nanocomposites of TPS-BNC10-GA, when compared with neat TPS, may be mainly associated with the presence of the BNC nanofibers that, despite their hydrophilic nature, are more crystalline. Moreover, as aforementioned, owing to the chemical similarity, the BNC nanofibers can establish interactions with starch matrix, resulting thereby in a good interfacial adhesion between both components, as evidenced by the SEM images and the enhanced mechanical strength. This, in turn, will reduce the diffusion of water molecules through the films similarly to what was observed by other authors for starch films reinforced with BNC nanofibers (Martins et al., 2009; Wan et al., 2009). From the results, it is also notorious that the GA had also a significant effect on the reduction of moisture absorption by the TPS-BNC-GA nanocomposites. This may be ascribed to the more hydrophobic nature of GA due to the aromatic ring (non-polar) in its structure (Galanakis et al., 2013), that will decrease the affinity of nanocomposites films for water molecules (Jaramillo et al., 2016). Hence, these results evidence the importance of adding, not only BNC nanofibers as reinforcement, but also GA to the plasticized starch matrix, to obtain nanocomposites with ameliorated resistance to ambient humidity.

3.5.2. *Water solubility*

Water solubility is another relevant characteristic that may give an indication about the water resistance properties of the developed nanocomposite films. Therefore, all the obtained TPS-based nanocomposites were tested for their solubility after 24 h of immersion in water. According to the results presented in Fig. 7B, the TPS film showed a solubility of 28.2 ± 7.1%, attributed to the dissolution of starch macromolecular fractions and glycerol, which agrees with values reported in literature for TPS films (Hu et al., 2009). In nanocomposites only with BNC, the solubility is similar to that of neat TPS, with values of 29.1 ± 1.7% for TPS-BNC1, 31.3 ± 1.3% for TPS-BNC5 and 26.7 ± 1.3% for TPS-BNC10, indicating that it will be the same fraction of starch and glycerol that is being dissolved. On the other hand, in the nanocomposite films incorporating GA and the two highest content of BNC nanofibers (5 and 10% w/w), it was observed a significant reduction in the solubility values, namely, to 21.6 ± 1.6% and 21.2 ± 2.5% for TPS-BNC5-GA1 and TPS-BNC5-GA1.5, respectively and 19.4 ±.1.2% for TPS-BNC10-GA1 and 18.0 ± 2.1% for TPS-BNC10-GA1.5. These findings are in line with the ones obtained in the moisture absorption assay and reinforce the importance of GA for improving the water resistance of nanocomposite films. As in moisture absorption, this effect is possibly associated with the non-polar aromatic ring of GA. In this way, the affinity of TPS matrix for water will be reduced and consequently its dissolution. These findings follow the same trend of reduction than those observed for starch-chitosan films loaded with green tea extract (Mangmee & Homthawornchoo, 2016).

Fig. 7C displays the visual appearance of the films before and after 24 h of immersion in water, showing that there was an alteration in the aspect of the TPS film immediately after immersion in water, whereas in the nanocomposites, the appearance is quite maintained even in the films with only 1% w/w of BNC nanofibers, suggesting the importance of this reinforcement for the cohesiveness of the films.

3.6. *Optical properties*

In packaging applications, transparency and UV-barrier properties can be especially relevant. Transparency is important for a good visualization of the products which can, in turn, interfere with consumers acceptance (Othman et al., 2019). A high barrier to UV radiation is also

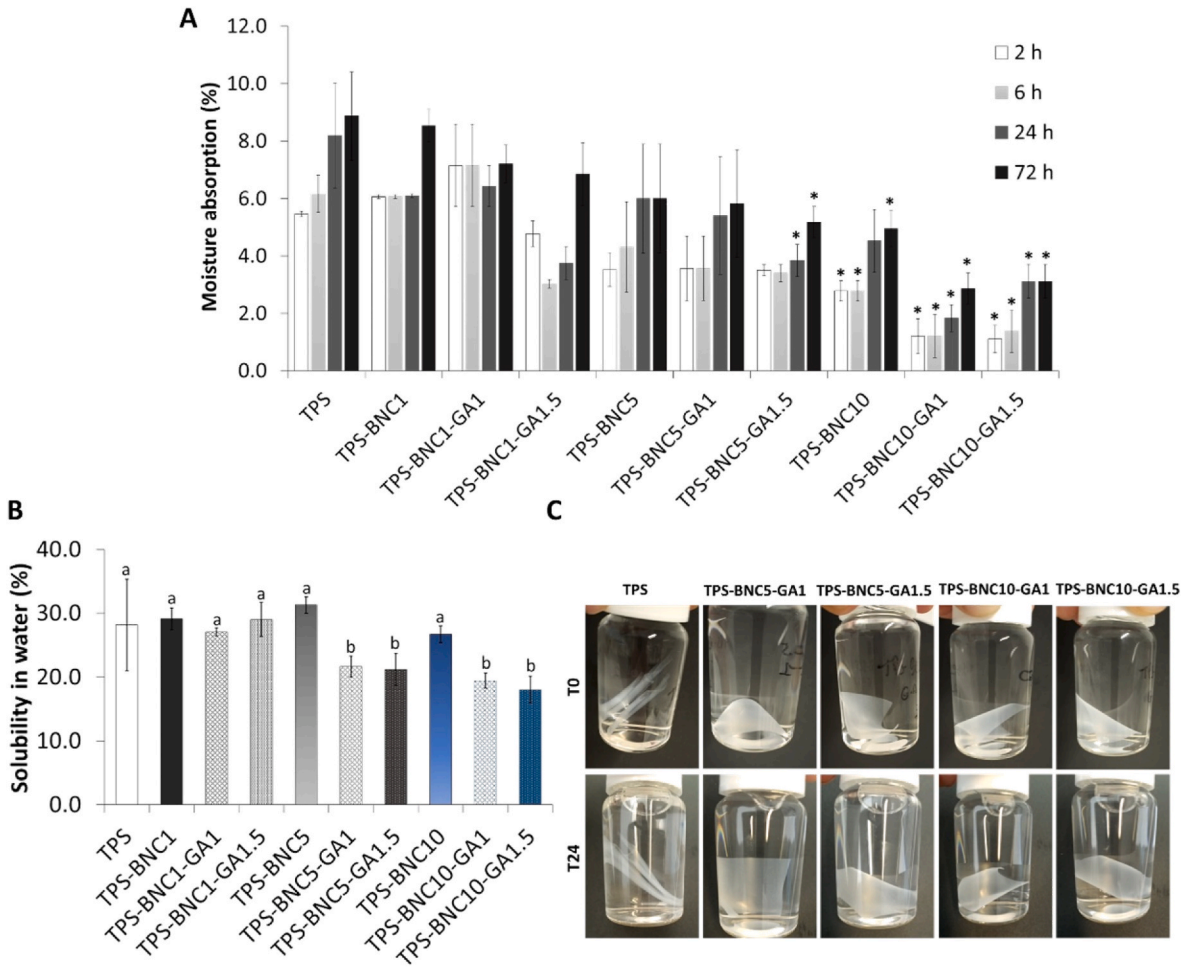

Fig. 7. (A) Moisture absorption at room temperature and 75% RH after 2 h, 6 h, 24 h and 72 h; and (B) Solubility in water of the TPS, TPS-BNC and of the TPS-BNC-GA nanocomposite films. The values are the mean of at least three replicates and the error bars correspond to standard deviations. In moisture absorption, for each time point, * denotes statistical differences ($p < 0.05$) against TPS film and in solubility, means with different letters indicate a significant difference ($p < 0.05$); (C) photographs of TPS films and of TPS-based nanocomposites whose solubility in water was significantly different from TPS.

desirable since it can prevent photodegradation of packed products, induced by photochemical reactions (Verduin, 2020). Hence, to have an insight about the optical properties of the prepared composite films, the transmittance spectrum in the UV–vis regions was acquired (Fig. 8A) and the opacity value was determined (Fig. 8B) for each film.

The transmittance spectra show that all TPS-based films are optically transparent with a transmittance varying between 77 and 89% in the visible region (400–800 nm), which concurs with their macroscopic appearance (Fig. 1). Despite the high values of transmittance, a small decrease in the transmittance of films with the increase in BNC nanofibers content was observed. But, even for the nanocomposites loaded with 10% w/w BNC nanofibers, the reduction in transmittance was only of about 10% compared with TPS, which still allows to easily see through them (Fig. 1). The effect of the BNC nanofibers on the transmittance of films was already observed in other biopolymeric films, based on chitosan (Fernandes et al., 2009), agar (Wang et al., 2018) or starch-chitosan (Abral et al., 2021). This reduction in transmittance is related to a higher quantity of light reflected and scattered in films with the increased nanofibers loadings (Abral et al., 2021).

The opacity of films was determined to evaluate the transparency of each film, considering that high opacity indicates low transparency (Wang et al., 2018). The opacity results (Fig. 8B) concur with the ones of transmittance, confirming that the transparency of films is reduced as the content of BNC nanofibers increases. While the neat TPS film showed an opacity value of 2.18 mm^{-1}, the nanocomposite films, have values varying between 2.24 mm^{-1} (TPS-BNC1) and 4.69 mm^{-1} (TPS-BNC10), with the films with 10% w/w of BNC nanofibers being the only ones with a significantly different opacity from the others (Fig. 8B). On the other hand, the incorporation of GA does not seem to have a considerable influence in the opacity of the films since, although slight variations are noted, these are not statistically significant. Zhao and Saldaña (2019) found that GA slight increase the transparency of starch films, but here this effect, especially in the nanocomposites with the higher content in BNC, may be masked by the presence of the nanofibers, resulting in less transparent films. However, the opacity values of the films with BNC contents below 10% w/w are in good agreement with the ones obtained for other biopolymeric-based films, such as for pectin films with 2.5% w/w of CNFs (2.40 ± 0.73 mm^{-1}) (Souza et al., 2022) or modified peanut protein films with 0.5–2% thymol (2.76–3.44 mm^{-1}) (Zhong et al., 2017). And, in the nanocomposites TPS-BNC10 and TPS-BNC10-GA, despite the increase in opacity, the values are lower than the ones attained for starch/CNFs films incorporated with thymol (Othman et al., 2021) or agar films with 10% of BNC (X. Wang et al., 2018). Moreover, it should also be emphasized that the opacity values here obtained are similar to the opacity of LDPE (3.05 mm^{-1}), which is classified as a transparent plastic and is widely applied in flexible packaging (Shiku et al., 2003).

Regarding the transmittance of the films in the UV-region, the spectra revealed that, while the TPS and TPS-BNC films displayed transmittance values between 48 and 87%, the GA-loaded counterparts

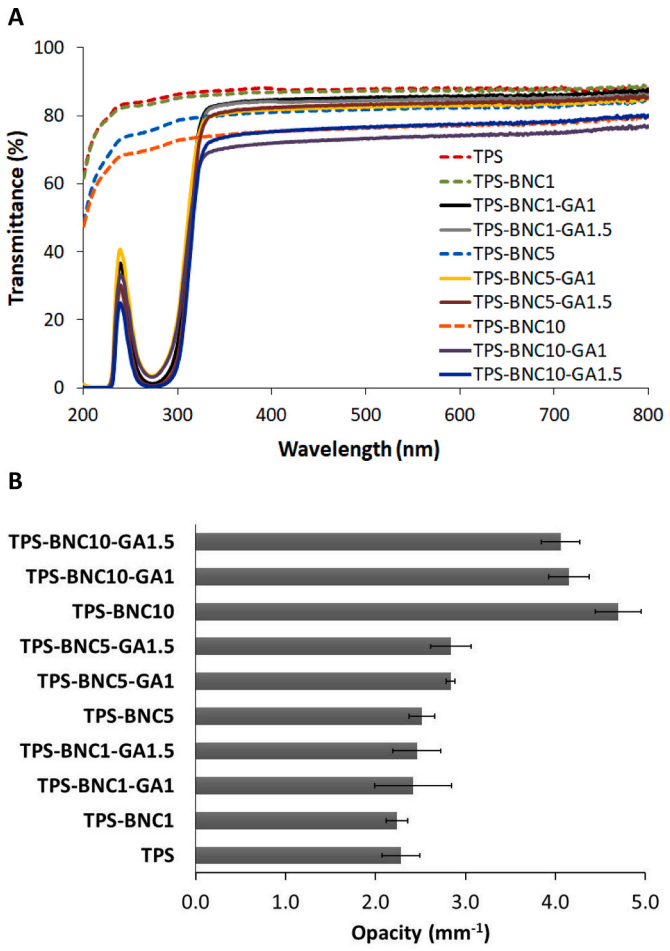

Fig. 8. (A) UV–vis transmission spectra and (B) opacity (A_{600}/mm) of the TPS film and of the TPS-based nanocomposite films with different contents of BNC and with different contents of BNC and GA. Means with different letters indicate a significant difference ($p < 0.05$).

have considerably lower transmittances with values between 0 and 60% in the range of 200–315 nm, indicating that these films have UV-barrier properties, in particular, in the UV-C (200–280 nm) and UV-B (280–315 nm) regions. The decrease in transmittance is related to the strong absorption of gallic acid in the UV-region due to the electronic transitions in the aromatic ring (Guo et al., 2021; Limpisophon & Schleining, 2017). Similar UV-blocking properties were observed in starch films loaded with tea polyphenols (Miao et al., 2021) or curcumin (Liu et al., 2022). As mentioned above, UV-radiation can catalyze various chemical reactions that, with a long-term exposure, can lead to organoleptic (e.g., color, flavor) changes, as well as lipid oxidation of oxidation-sensitive substances which in turn can also lead to organoleptic alterations (Verduin, 2020). Therefore, the incorporation of GA in the TPS-BNC nanocomposite films opens the possibility of using these active films as UV-absorbent materials with the ability to prevent light-degradation of light-sensitive food (e.g., nuts, fruits, vegetables) that may be more attractive for the consumer if packaged with transparent materials.

3.7. Antioxidant activity

The deterioration of susceptible products to oxidative degradation, like fat-containing food, can be reduced by the incorporation of antioxidants into the packaging materials (Carvalho et al., 2021; Laguerre et al., 2007; Vilela et al., 2018). The incorporation of antioxidants into the packaging material (viz. active packaging) is growing and is now seen as a viable and attractive alternative when compared to the direct addition of antioxidants to the packed products, since it allows to circumvent problems related to organoleptic alterations (Carvalho et al., 2021). As abovementioned, GA is a natural compound that has demonstrated a potent antioxidant activity, owing to the multiple hydroxyl groups present in its molecular structure (Jing et al., 2012). Hence, the antioxidant activity of the prepared films was evaluated by the DPPH radical scavenging assay. The results presented in Fig. 9 show that, as predicted, in films without GA (TPS and TPS-BNC) no antioxidant activity was observed. On the contrary, all TPS-BNC-GA films, regardless of the GA concentration, exhibited a DPPH scavenging activity of around 85%, confirming that this compound has conferred antioxidant capacity to the TPS matrix, similar to what was previously reported for films of gelatin (Limpisophon & Schleining, 2017) or chitosan (Kaczmarek-Szczepańska et al., 2022). These findings confirmed the potential of the TPS-BNC-GA films as active packaging material for products susceptible to oxidative degradation.

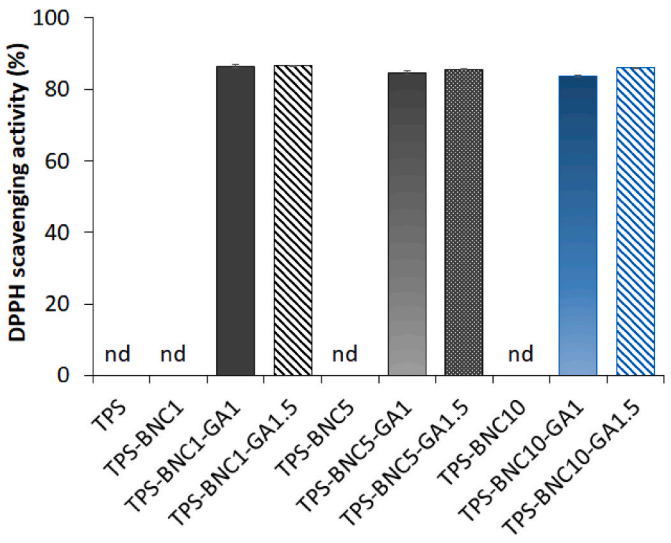

Fig. 9. Antioxidant activity of the TPS film and of the TPS-based nanocomposite films with different contents of BNC and of GA. Results are expressed as means of three independent assays and the error bars correspond to standard deviations; nd – not detected.

3.8. Oxygen permeability

The oxygen permeability rate is considered one of the most relevant properties in the development of a packaging material. Oxygen is responsible for causing lipid oxidation, vitamin degradation and by facilitating the development of aerobic microorganisms, the most implied microorganisms in food spoilage (Michiels et al., 2017). Therefore, for certain products in order to maximize their shelf-life and to guarantee the preservation of their properties and the safety of the consumer, is essential that the packaging material has a low oxygen permeability rate. In this sense, the oxygen permeability (OP) coefficient of the film TPS-BNC10-GA1 as well as of the TPS and TPS-BNC10 films, as blank references, was determined. The TPS-BNC10-GA1 film was selected for this evaluation taking into account the characterization results, namely opacity, mechanical resistance, thermal stability and water resistance, and antioxidant activity, in which, no significant differences were detected among the nanocomposites containing GA. Therefore, as a lower amount of GA is added to this formulation, this was selected considering a possible scale up in the future. The results (Table 2) clearly show that, with the addition of BNC nanofibers, the oxygen permeability rates of the composite films were considerably reduced (~8 times) compared to the permeability of the pure TPS film. This effect is probably related to the fact that the BNC nanofibers, by having a crystalline nature, represent a dispersed phase in the starch

Table 2
Oxygen permeability coefficient (OP) of the TPS, TPS-BNC10 and TPS-BNC10-GA1 nanocomposite films.

Film	Oxygen Permeability Coefficient (cm^3 µm m^{-2} d^{-1} kPa^{-1})
TPS	8.00 ± 3.00
TPS-BNC10	1.00 ± 0.00
TPS-BNC10-GA1	0.91 ± 0.12

matrix, thus creating a tortuous path, which hinders the diffusion of oxygen molecules and reduces their passage per unit of time (Lagaron et al., 2004). A similar effect was described for cassava starch films reinforced with 3% w/w of microcrystalline cellulose (Othman et al., 2019) and for TPS films with 0.4% w/w of cellulose nanofibers (Fazeli et al., 2018). The addition of GA also had a positive effect on reducing the permeability of the films to oxygen, possibly due to the establishment of interactions with TPS and BNC that hinders the diffusion of gas molecules (Singh et al., 2022). It should be noted that the oxygen permeability coefficient of the TPS-BNC10-GA1 nanocomposite film (0.91 cm^3 µm m^{-2} d^{-1} kPa^{-1}) is considerably lower than the values described for synthetic polymers used in flexible packaging, such as LDPE (2.74–3.60 cm^3 µm m^{-2} d^{-1} kPa^{-1}) (Mangaraj, Goswami, & Mahajan, 2009), meaning that the TPS-BNC10-GA1 nanocomposite has a better performance in what concerns the oxygen barrier and that it is comparable to values reported for the EVOH (0.08–0.31 cm^3 µm m^{-2} d^{-1} kPa^{-1} 23 °C, 65% RH) another synthetic polymer widely used (Maes et al., 2018). This indicates thereby that, for the nanocomposite TPS-BNC10-GA1, a good oxygen barrier was achieved and kept at both technically and commercially appropriate levels for the intended application.

3.9. In vitro antibacterial activity

Food products (e.g., meat, smoked fish, vegetables) are susceptible to microbial contamination by spoilage microorganisms and/or pathogenic microorganisms, that can cause their deterioration and compromise thereby the consumer safety (Vilela et al., 2018; Yildirim et al., 2018). In this field, the incorporation of antimicrobial agents in the packaging material has been explored as a successful strategy to preserve the quality and extend the shelf-life of products (Kamarudin et al., 2022). Therefore, herein the antibacterial activity of the developed TPS-based nanocomposites enriched with GA was assessed against the Gram-positive *S. aureus,* which is one of the major pathogenic bacteria responsible for food spoilage, frequently involved in food-borne illness (Paiva et al., 2021). As aforementioned, based on the overall results of characterization and, in particular, those of antioxidant activity, only the TPS-BNC10-GA1 film and the TPS and the TPS-BNC10 films (as blank references) were evaluated in this assay.

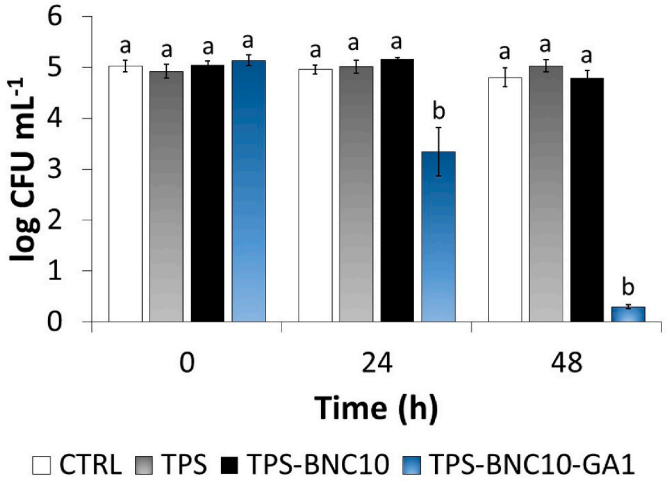

Fig. 10. Antibacterial activity of TPS, TPS-BNC10 and TPS-BNC10-GA1 nanocomposite films towards *S. aureus* MRSA DSM 25693 after 24 h and 48 h. Results are expressed as means of three independent assays and error bars correspond to standard deviations. Means with different letters indicate a significant difference ($p < 0.05$).

The results depicted in Fig. 10 confirmed that after 48 h, the films without GA (TPS and TPS-BNC10) did not cause any reduction in the initial bacterial concentration, having indeed an identical profile to the one observed for the bacterial control (CTRL). This concurs with results obtained by other authors for TPS films and TPS films with BNC regarding the antibacterial activity against *S. aureus* (Abral et al., 2021; López et al., 2020). On the contrary, the film enriched with GA (TPS-BNC10-GA1) lead to a significant decrease in the initial bacterial concentration of ~1.6-log_{10} CFU mL^{-1} after 24 h and of ~4.5-log_{10} CFU mL^{-1} after 48 h, thus indicating that, the film has a bactericidal effect against the *S. aureus*, since a reduction superior to 3-log_{10} CFU mL^{-1}, in the initial inoculum, was attained after 48 h (Glueck et al., 2017). The mechanism of action of GA is reported to be associated with the hyper-acidification of cytoplasm due to the diffusion of GA through cell membrane. This intracellular acidification can alter the potential of cell membrane and turn it more permeable, causing thereby irreversible changes that lead to cell death (Borges et al., 2013). The antibacterial activity against *S. aureus* of GA was already verified when incorporated in blends of konjac glucomannan and gellan gum (Du et al., 2019) or chitosan and poly(vinyl alcohol) (Yoon et al., 2017). However, this is the first time that this effect of GA is described in association with TPS-BNC nanocomposite.

Thus, these results have proved that the developed nanocomposites have antibacterial activity, which emphasizes their potential to be applied in active food packaging.

3.10. Films performance on preserving fresh-cut apple

Considering the results obtained so far, particularly, for the antioxidant activity and oxygen permeability of the nanocomposite films, the performance of the TPS-BNC10-GA1 film, as well as of the TPS, TPS-BNC10 and commercial LDPE for comparison, when applied in the packaging of a real food matrix was evaluated. In this regard, minimally processed fresh-cut apple samples, known to be rich in polyphenols and highly susceptible to oxidation (Shrestha et al., 2020), were packaged, stored for 7 days at +4 ± 1 °C and evaluated over time for several parameters (BI, weight loss, and pH) associated with fruit quality and acceptance of consumers (Jancikova et al., 2021; Jiang et al., 2021).

The BI of packaged fresh-cut apple are depicted in Fig. 11A. Before storage, apples samples had a BI of 31.6 ± 0.9. But, after 7 days of storage at 4 ± 1 °C, the BI of all fresh-cut apple samples increased. However, it is notorious that the TPS-BNC10-GA1 nanocomposite film had a positive effect in delaying the browning of the packaged fresh-cut apples, that showed a BI value of 52.2 ± 1.0, while apples packaged with the LDPE commercial film exhibited a BI of 95.5 ± 1.8. If compared with TPS (63.0 ± 1.5) and TPS-BNC10 (60.6 ± 1.1), eventhough the difference is not so pronounced, the value is still considerably lower ($p < 0.05$). This result agrees with the visual appearance (Fig. 11B) of the packaged fresh-cut apples after 7 days of storage. One cause of fruit browning is the enzymatic browning, resulting from the oxidation reaction of polyphenols catalysed by the polyphenol oxidase (PPO), producing o-quinones that are then polymerized with other quinones and amines to generate brown pigments (Shrestha et al., 2020). Thus, since antioxidants are described as chemical inhibitors of PPO activity (Moon et al., 2020), the antioxidant capability of the TPS-BNC10-GA1 film, imparted by the presence of GA, is probably one of the main factors contributing to reduce the browning of fresh-cut apple. A similar effect was also observed by other authors when fresh-cut apples were packaged with chitosan/guar film containing an antioxidant walnut green husk extract (Jiang et al., 2022). Moreover, the superior oxygen barrier

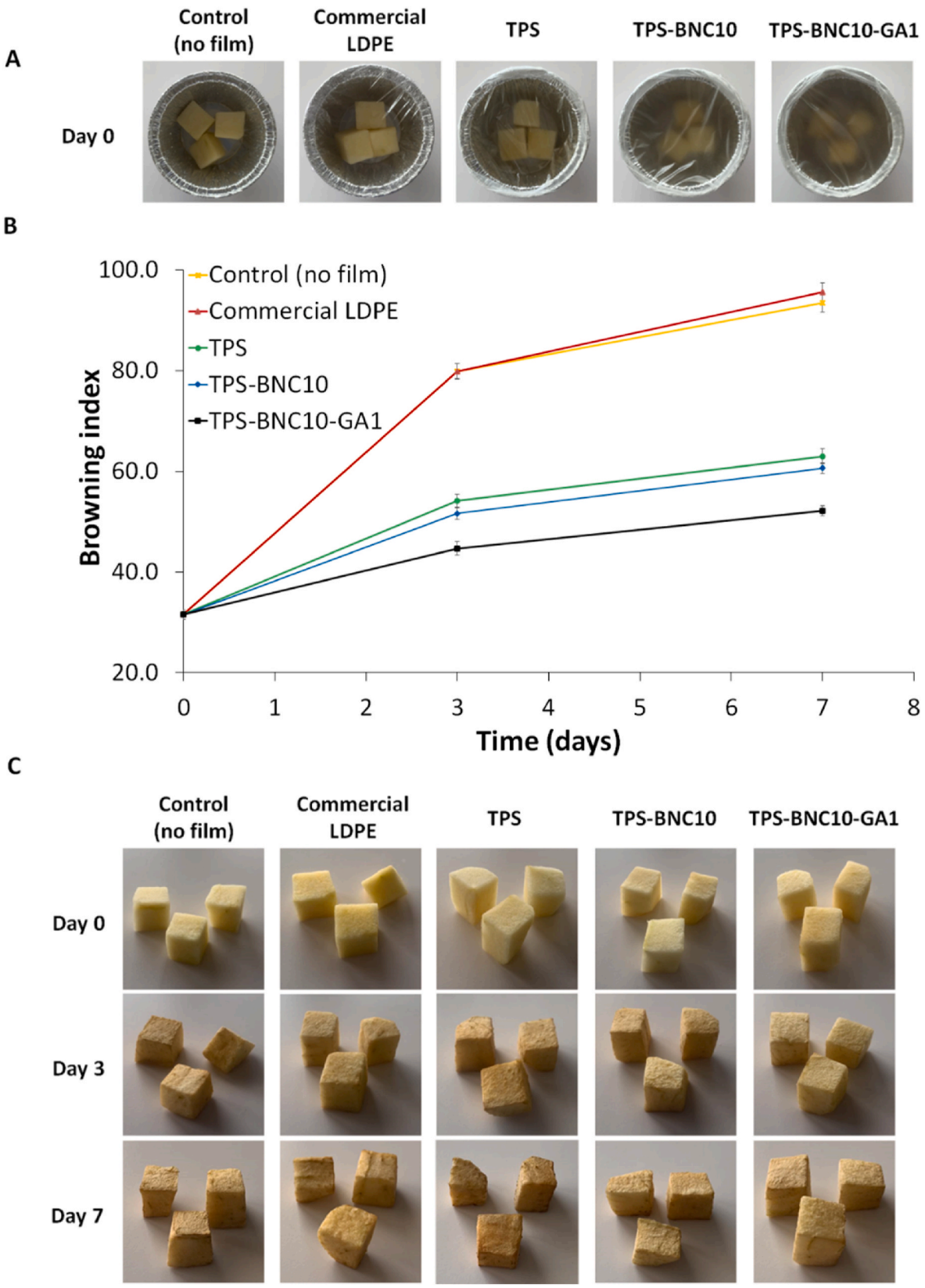

Fig. 11. (A) Digital photographs of the packaged fruits with the different films at day 0 (B) BI and (C) physical appearance of fresh-cut apples before and after storage at +4 °C for 3 and 7 days with no film or packaged with different films (LDPE commercial film, TPS, TPS-BNC10 and TPS-BNC10-GA1).

property of TPS-BNC10-GA1 film compared with the other tested films, including LDPE, further reduce the oxygen that enters inside the packaging, which is necessary to initiate the conversion of phenols into quinones (Moon et al., 2020), thus contributing to prevent the browning of fresh-cut apple samples.

With regard to weight loss of fresh-cut apples over storage time (Fig. 12A), results evidence that through the 7 days, all samples showed an upward trend of losing weight as previously described by other authors for fresh-cut apples packaged with chitosan/guar film containing walnut green husk extract (Jiang et al., 2022) or chitosan/gelatin-based films loaded with tannic acid (Zhang et al., 2021). In the present study, fresh-cut apples packaged without film (control) showed the highest weight loss (36.0 ± 0.6%) and those packaged with commercial LDPE, exhibited the lowest weight loss (5.9 ± 0.5%) at day 7. At this storage point, apple samples packaged with the TPS-BNC10-GA1 film, lost about 24.0 ± 0.6% of their weight, similarly to the value obtained for fresh-cut samples in TPS-BNC10 film (24.2 ± 0.8). The observed weight loss in all samples is probably associated with the immediate increase in respiration rate after cutting, with consequent rise in water and nutrient consumption that will in turn cause the weight loss (Guan et al., 2023).

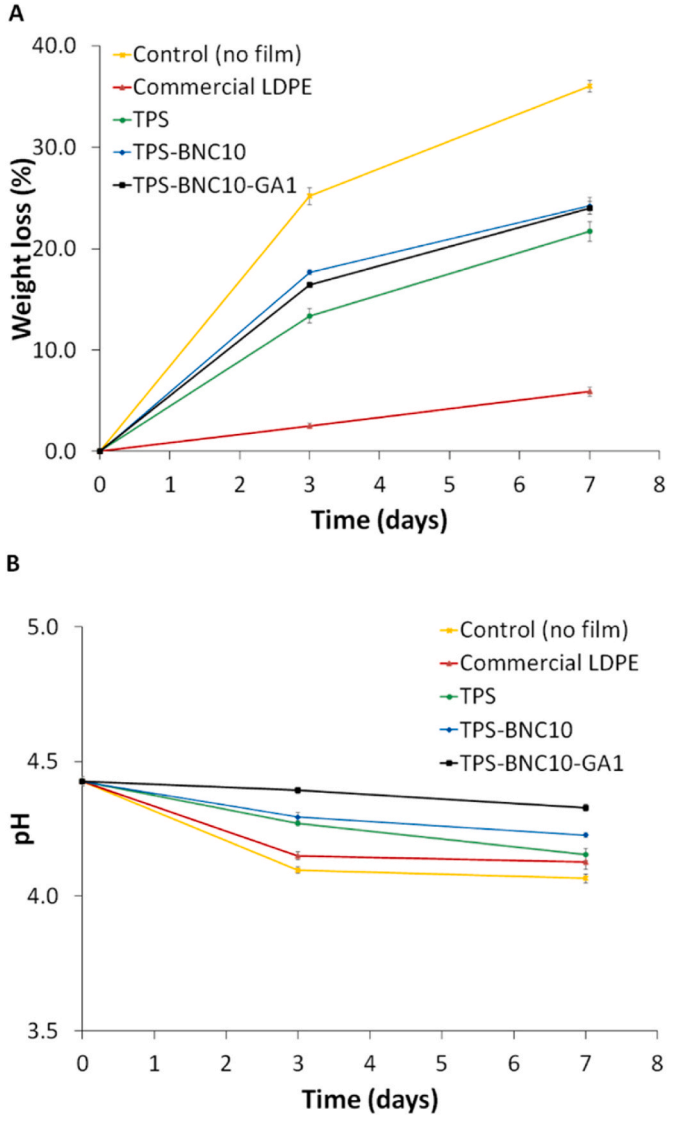

Fig. 12. (A) Weight loss percentage (%) and (B) pH evolution of minimally processed apple samples before and after storage at +4 °C for 3 and 7 days with no film or packed with different films (LDPE commercial film, TPS, TPS-BNC10 and TPS-BNC10-GA1).

In Fig. 12B is also shown the evolution of pH of the fresh-cut samples during storage, revealing that over time. The initial pH of apple samples was 4.43 ± 0.02, and after 7 days at 4 °C, the pH was 4.07 ± 0.02. In all the other samples, a significant decrease ($p < 0.05$) in pH had also occurred, with the TPS-BNC10-GA1 nanocomposite film showing the lowest decrease (pH: 4.33 ± 0.01) comparatively ($p < 0.05$) with the other tested films (LDPE: 4.13 ± 0.03; TPS: 4.15 ± 0.02; TPS-BNC10: 4.23 ± 0.01), suggesting a better performance of the developed films in keeping the value of pH from the packaged fruit.

Therefore, the overall results of this evaluation, using a real food matrix, demonstrate the applicability of the developed nanocomposites films to preserve minimally processed fresh-cut apple at 4 °C, showing an especially superior performance in preventing the browning of the fruit, which is a critical aspect to maintain the quality and consumer acceptance.

4. Conclusions

Bioactive TPS nanocomposite films, reinforced with different contents of BNC nanofibers and enriched with GA were developed. In terms of mechanical properties, the reinforcement of the TPS matrix with the BNC nanofibers and the addition of GA led to an increase in the strength (YM and TS) of the films and, despite a reduction in elasticity, they remained flexible and handleable enough for the target application. The inclusion of BNC nanofibers and GA into the TPS matrix also increased the resistance of films to both moisture absorption and water solubility, properties that often limit the application of starch as a packaging material. Furthermore, the ensuing films were visually transparent and had a transmittance in the visible region close to 80% and opacity values comparable to those of LDPE films. With the addition of GA, films were also imparted with UV-absorbing properties and with antioxidant capacity, which are highly valued by the packaging sector. The film with 10% w/w of BNC and 1% w/w of GA was then selected for further characterization in terms of oxygen permeability barrier and antibacterial activity, showing that this formulation exhibited a good oxygen barrier, comparable to the one of the EVOH, widely applied in flexible packaging applications. In addition, results also showed that GA has conveyed the film with antibacterial activity against the Gram-positive *S. aureus* bacteria, being the first time that this activity is reported for TPS-BNC composites, which reinforces the novelty of this work. The potential of the film with 10% w/w of BNC and 1% w/w of GA was additionally assessed by testing it in the packaging of fresh-cut apple stored at 4 °C for 7 days, showing that this nanocomposite film has a superior performance with respect to delaying the browning and weight loss of fresh-cut apple when compared with commercial LDPE, TPS and TPS-BNC10 films. In light of the obtained results, it is suggested that the developed TPS-BNC-GA nanocomposite films, combining these two hydrocolloid biopolymers with GA, are good candidates to be explored as innovative flexible, sustainable and eco-friendly active packaging materials.

Credit authorship statement

Tânia Almeida: Investigation; Writing - original draft; Anna Karamysheva: Investigation; Writing - review & editing. Bruno F. A. Valente: Investigation; Writing - review & editing. José M. Silva: Investigation; Writing - review & editing. Márcia Braz: Investigation; Writing - review & editing. Adelaide Almeida: Funding acquisition; Resources; Writing - review & editing. Armando J. D. Silvestre: Funding acquisition; Resources; Writing - review & editing. Carla Vilela: Funding acquisition; Supervision; Writing - review & editing. Carmen S.R. Freire: Conceptualization; Funding acquisition; Project administration; Resources; Supervision; Writing - review & editing.

Funding

This work was carried out under the Project inpactus – innovative products and technologies from eucalyptus, Project N° 21874 funded by Portugal 2020 through European Regional Development Fund (ERDF) in the frame of COMPETE 2020 n°246/AXIS II/2017, project CICECO – Aveiro Institute of Materials, UIDB/50011/2020, UIDP/50011/2020 & LA/P/0006/2020, and project CESAM, UIDP/50017/2020 and UIDB/50017/2020 and LA/P/0094/2020, financed by national funds through the FCT/MCTES (PIDDAC). FCT is also acknowledged for the research contracts under Scientific Employment Stimulus to C.V. (CEECIND/00263/2018 and 2021.01571. CEECIND) and C.S.R.F. (CEECIND/00464/2017).

Declaration of competing interest

The authors declare that they have no known competing financial interests or personal relationships that could have appeared to influence the work reported in this paper.

Data availability

All data was included in the manuscript.

References

Abdullah, A. H. D., Chalimah, S., Primadona, I., & Hanantyo, M. H. G. (2018). Physical and chemical properties of corn, cassava, and potato starchs. *IOP Conference Series: Earth and Environmental Science, 160*(1), Article 012003. https://doi.org/10.1088/1755-1315/160/1/012003

Abral, H., Pratama, A. B., Handayani, D., Mahardika, M., Aminah, I., Sandrawati, N., & Ilyas, R. A. (2021). Antimicrobial edible film prepared from bacterial cellulose nanofibers/starch/chitosan for a food packaging alternative, 2021 *International Journal of Polymer Science*. , Article 6641284. https://doi.org/10.1155/2021/6641284.

Almeida, T., Moreira, P., Sousa, F. J., Pereira, C., Silvestre, A. J. D., Vilela, C., & Freire, C. S. R. (2022). Bioactive bacterial nanocellulose membranes enriched with Eucalyptus globulus Labill. Leaves aqueous extract for anti-aging skin care applications, 1982 *Materials, 15*(5). https://doi.org/10.3390/ma15051982.

Badhani, B., Sharma, N., & Kakkar, R. (2015). Gallic acid: A versatile antioxidant with promising therapeutic and industrial applications. *RSC Advances, 5*(35), 27540–27557. https://doi.org/10.1039/c5ra01911g

Bodîrlău, R., Teacă, C.-A., & Spiridon, I. (2014). Starch-cellulose composites. *Bioresources, 9*(1), 39–53.

Borges, A., Ferreira, C., Saavedra, M. J., & Simões, M. (2013). Antibacterial activity and mode of action of ferulic and gallic acids against pathogenic bacteria. *Microbial Drug Resistance, 19*(4), 256–265. https://doi.org/10.1089/mdr.2012.0244

Cacicedo, M. L., Castro, M. C., Servetas, I., Bosnea, L., Boura, K., Tsafrakidou, P., & Castro, G. R. (2016). Progress in bacterial cellulose matrices for biotechnological applications. *Bioresource Technology, 213*, 172–180. https://doi.org/10.1016/j.biortech.2016.02.071

Carvalho, J., Freire, C. S. R., & Vilela, C. (2021). Active packaging (chapter 9). In C. M. Galanakis (Ed.), *Sustainable food packaging and engineering challenges* (1st ed., pp. 315–334). Academic Press.

Cavaliere, A., Pigliafreddo, S., de Marchi, E., & Banterle, A. (2020). Do consumers really want to reduce plastic usage? Exploring the determinants of plastic avoidance in food-related consumption decisions. *Sustainability, 12*(22), 1–15. https://doi.org/10.3390/su12229627

Chen, H., Alee, M., Chen, Y., Zhou, Y., Yang, M., Ali, A., & Yu, L. (2021). Developing edible starch film used for packaging seasonings in instant noodles. *Foods, 10*(12), 3105. https://doi.org/10.3390/foods10123105

Chen, N., Gao, H. X., He, Q., Yu, Z. L., & Zeng, W. C. (2020). Interaction and action mechanism of starch with different phenolic compounds. *International Journal of Food Sciences & Nutrition, 71*(6), 726–737. https://doi.org/10.1080/09637486.2020.1722074

Cheng, H., Chen, L., McClements, D. J., Yang, T., Zhang, Z., Ren, F., & Jin, Z. (2021). Starch-based biodegradable packaging materials: A review of their preparation, characterization and diverse applications in the food industry. *Trends in Food Science and Technology, 114*, 70–82. https://doi.org/10.1016/j.tifs.2021.05.017

Chiozzi, V., Agriopoulou, S., & Varzakas, T. (2022). Advances, applications, and comparison of thermal (pasteurization, sterilization, and aseptic packaging) against non-thermal (ultrasounds, UV radiation, ozonation, high hydrostatic pressure) technologies in food processing. *Applied Sciences, 12*(4), 2202. https://doi.org/10.3390/app12042202

Compart, J., Li, X., & Fettke, J. (2021). Starch-A complex and undeciphered biopolymer, 153389 *Journal of Plant Physiology*, 258–259. https://doi.org/10.1016/j.jplph.2021.153389.

Costa, A. F. S., Almeida, F. C. G., Vinhas, G. M., & Sarubbo, L. A. (2017). Production of bacterial cellulose by Gluconacetobacter hansenii using corn steep liquor as nutrient sources. *Frontiers in Microbiology, 8*, 2027. https://doi.org/10.3389/fmicb.2017.02027

Du, Y., Sun, J., Wang, L., Wu, C., Gong, J., Lin, L., & Pang, J. (2019). Development of antimicrobial packaging materials by incorporation of gallic acid into Ca^{2+} crosslinking konjac glucomannan/gellan gum films. *International Journal of Biological Macromolecules, 137*, 1076–1085. https://doi.org/10.1016/j.ijbiomac.2019.06.079

Fabra, J. M., López-Rubio, A., & Ambrosio-Martín, J. (2016). Improving the barrier properties of thermoplastic corn starch-based films containing bacterial cellulose nanowhiskers by means of PHA electrospun 2 coatings of interest in food packaging. *Food Hydrocolloids, 61*, 261–268.

Fazeli, M., Keley, M., & Biazar, E. (2018). Preparation and characterization of starch-based composite films reinforced by cellulose nanofibers. *International Journal of Biological Macromolecules, 116*, 272–280. https://doi.org/10.1016/j.ijbiomac.2018.04.186

Fernandes, S. C. M., Oliveira, L., Freire, C. S. R., Silvestre, A. J. D., Neto, C. P., Gandini, A., & Desbriéres, J. (2009). Novel transparent nanocomposite films based on chitosan and bacterial cellulose. *Green Chemistry, 11*(12), 2023–2029. https://doi.org/10.1039/b919112g

Ferreira-Santos, P., Genisheva, Z., Pereira, R. N., Teixeira, J. A., & Rocha, C. M. R. (2019). Moderate electric fields as a potential tool for sustainable recovery of phenolic compounds from Pinus pinaster bark. *ACS Sustainable Chemistry & Engineering, 7*(9), 8816–8826. https://doi.org/10.1021/acssuschemeng.9b00780

Galanakis, C. M., Goulas, V., Tsakona, S., Manganaris, G. A., & Gekas, V. (2013). A knowledge base for the recovery of natural phenols with different solvents. *International Journal of Food Properties, 16*(2), 382–396. https://doi.org/10.1080/10942912.2010.522750

García-Guzmán, L., Cabrera-Barjas, G., Soria-Hernández, C. G., Castaño, J., Guadarrama-Lezama, A. Y., & Rodríguez Llamazares, S. (2022). Progress in starch-based materials for food packaging applications. *Polysaccharides, 3*(1), 136–177. https://doi.org/10.3390/polysaccharides3010007

Glueck, M., Schamberger, B., Eckl, P., & Plaetzer, K. (2017). New horizons in microbiological food safety: Photodynamic Decontamination based on a curcumin derivative. *Photochemical and Photobiological Sciences, 16*(12), 1784–1791. https://doi.org/10.1039/c7pp00165g

Gomes, F. P., Silva, N. H. C. S., Trovatti, E., Serafim, L. S., Duarte, M. F., Silvestre, A. J. D., & Freire, C. S. R. (2013). Production of bacterial cellulose by Gluconacetobacter sacchari using dry olive mill residue. *Biomass and Bioenergy, 55*, 205–211. https://doi.org/10.1016/j.biombioe.2013.02.004

González, K., Iturriaga, L., González, A., Eceiza, A., & Gabilondo, N. (2020). Improving mechanical and barrier properties of thermoplastic starch and polysaccharide nanocrystals nanocomposites. *European Polymer Journal, 123*, Article 109415. https://doi.org/10.1016/j.eurpolymj.2019.109415

Grande, C., Torres, F., Gomez, C., Troncoso, O., Cane-Ferrer, J., & Martinez-Pastor, J. (2008). Morphological characterisation of bacterial cellulose-starch nanocomposites. *Polymers and Polymer Composites, 16*(3), 181–185.

Greenspan, L. (1977). Humidity fixed points of binary saturated aqueous solutions. *Journal of Research of the National Bureau of Standards-A. Phys Ics and Chemistry, 81*(1).

Guan, Y., Ji, Y., Yang, X., Pang, L., Cheng, J., Lu, X., & Hu, W. (2023). Antioxidant activity and microbial safety of fresh-cut red cabbage stored in different packaging films. *LWT, 175*. https://doi.org/10.1016/j.lwt.2023.114478

Guillard, V., Gaucel, S., Fornaciari, C., Angellier-Coussy, H., Buche, P., & Gontard, N. (2018). The next generation of sustainable food packaging to preserve our environment in a circular economy context. *Frontiers in Nutrition, 5*, 121. https://doi.org/10.3389/fnut.2018.00121

Guo, L., Qiang, T., Ma, Y., Ren, L., & Zhu, C. (2021). Biodegradable anti-ultraviolet film from modified gallic acid cross-linked gelatin. *ACS Sustainable Chemistry & Engineering, 9*, 8393–8401. https://doi.org/10.1021/acssuschemeng.1c00085

Hafizulhaq, F., Abral, H., Kasim, A., Arief, S., & Affi, J. (2018). Moisture absorption and opacity of starch-based biocomposites reinforced with cellulose fiber from bengkoang. *Fibers, 6*(3), 62. https://doi.org/10.3390/fib6030062

Hu, G., Chen, J., & Gao, J. (2009). Preparation and characteristics of oxidized potato starch films. *Carbohydrate Polymers, 76*(2), 291–298. https://doi.org/10.1016/j.carbpol.2008.10.032

Jancikova, S., Dordevic, D., Tesikova, K., Antonic, B., & Tremlova, B. (2021). Active edible films fortified with natural extracts: Case study with fresh-cut apple pieces. *Membranes, 11*(9). https://doi.org/10.3390/membranes11090684

Jaramillo, C. M., Gutiérrez, T. J., Goyanes, S., Bernal, C., & Famá, L. (2016). Biodegradability and plasticizing effect of yerba mate extract on cassava starch edible films. *Carbohydrate Polymers, 151*, 150–159. https://doi.org/10.1016/j.carbpol.2016.05.025

Jiang, L., Wang, F., Xie, X., Xie, C., Li, A., Xia, N., & Zhang, H. (2022). Development and characterization of chitosan/guar gum active packaging containing walnut green husk extract and its application on fresh-cut apple preservation. *International Journal of Biological Macromolecules, 209*, 1307–1318. https://doi.org/10.1016/j.ijbiomac.2022.04.145

Jiang, T., Duan, Q., Zhu, J., Liu, H., & Yu, L. (2020). Starch-based biodegradable materials: Challenges and opportunities. *Advanced Industrial and Engineering Polymer Research, 3*(1), 8–18. https://doi.org/10.1016/j.aiepr.2019.11.003

Jiang, L., Luo, Z., Liu, H., Wang, F., Li, H., Gao, H., & Zhang, H. (2021). Preparation and characterization of chitosan films containing lychee (Litchi chinensis sonn.) pericarp powder and their application as active food packaging. *Foods, 10*(11). https://doi.org/10.3390/foods10112834

Jildeh, Z. B., Wagner, P. H., & Schöning, M. J. (2021). Sterilization of objects, products, and packaging surfaces and their characterization in different fields of industry: The status in 2020. *Physica Status Solidi (A) Applications and Materials Science, 218*(13), Article 2000732. https://doi.org/10.1002/pssa.202000732

Jing, P., Zhao, S. J., Jian, W. J., Qian, B. J., Dong, Y., & Pang, J. (2012). Quantitative studies on Structure-DPPH· scavenging activity relationships of food phenolic acids. *Molecules, 17*(11), 12910–12924. https://doi.org/10.3390/molecules171112910

Kaczmarek-Szczepańska, B., Zasada, L., & Grabska-Zielińska, S. (2022). The physicochemical, antioxidant, and color properties of thin films based on chitosan modified by different phenolic acids. *Coatings, 12*(2), 126. https://doi.org/10.3390/coatings12020126

Kamarudin, S. H., Rayung, M., Abu, F., Ahmad, S., Fadil, F., Karim, A. A., & Abdullah, L. C. (2022). A review on antimicrobial packaging from biodegradable polymer composites. *Polymers, 14*(1), 174. https://doi.org/10.3390/polym14010174

Karimi, S., Tahir, P. M., Dufresne, A., Karimi, A., & Abdulkhani, A. (2014). A comparative study on characteristics of nanocellulose reinforced thermoplastic starch biofilms prepared with different techniques. *Nordic Pulp and Paper Research Journal, 29*(1), 2014.

Khan, B., Bilal Khan Niazi, M., Samin, G., & Jahan, Z. (2017). Thermoplastic starch: A possible biodegradable food packaging material—a review. *Journal of Food Process Engineering, 40*(3), Article e12447. https://doi.org/10.1111/jfpe.12447

Klemm, D., Kramer, F., Moritz, S., Lindström, T., Ankerfors, M., Gray, D., & Dorris, A. (2011). Nanocelluloses: A new family of nature-based materials. *Angewandte Chemie International Edition in English, 50*(24), 5438–5466. https://doi.org/10.1002/anie.201001273

Kumar, V., Sharma, D. K., Bansal, V., Mehta, D., Sangwan, R. S., & Yadav, S. K. (2019). Efficient and economic process for the production of bacterial cellulose from isolated strain of Acetobacter pasteurianus of RSV-4 bacterium. *Bioresource Technology, 275*, 430–433. https://doi.org/10.1016/j.biortech.2018.12.042

Lagaron, J. M., Catalá, R., & Gavara, R. (2004). Structural characteristics defining high barrier properties in polymeric materials. *Materials Science and Technology, 20*(1), 1–7. https://doi.org/10.1179/026708304225010442

Laguerre, M., Lecomte, J., & Villeneuve, P. (2007). Evaluation of the ability of antioxidants to counteract lipid oxidation: Existing methods, new trends and challenges. *Progress in Lipid Research, 46*(Issue 5), 244–282. https://doi.org/10.1016/j.plipres.2007.05.002

Lauer, M. K., & Smith, R. C. (2020). Recent advances in starch-based films toward food packaging applications: Physicochemical, mechanical, and functional properties. *Comprehensive Reviews in Food Science and Food Safety, 19*(6), 3031–3083. https://doi.org/10.1111/1541-4337.12627

Limpisophon, K., & Schleining, G. (2017). Use of gallic acid to enhance the antioxidant and mechanical properties of active fish gelatin film. *Journal of Food Science, 82*(1), 80–89. https://doi.org/10.1111/1750-3841.13578

Liu, Y., Liu, M., Zhang, L., Cao, W., Wang, H., Chen, G., & Wang, S. (2022). Preparation and properties of biodegradable films made of cationic potato-peel starch and loaded with curcumin. *Food Hydrocolloids, 130*, Article 107690. https://doi.org/10.1016/j.foodhyd.2022.107690

López, O.v., Villanueva, M. E., Copello, G. J., & Villar, M. A. (2020). Flexible thermoplastic starch films functionalized with copper particles for packaging of food products. *Functional Composite Materials, 1*(1), 1–6. https://doi.org/10.1186/s42252-020-00009-7

Luo, Y., Wu, Y., Wang, Y., & Yu, L. (2021). Active and robust composite films based on gelatin and gallic acid integrated with microfibrillated cellulose. *Foods, 10*(11), 2831. https://doi.org/10.3390/foods10112831

Luzi, F., Torre, L., Kenny, J. M., & Puglia, D. (2019). Bio- and fossil-based polymeric blends and nanocomposites for packaging: Structure-property relationship. *Materials, 12*(3), 471. https://doi.org/10.3390/ma12030471

Maes, C., Luyten, W., Herremans, G., Peeters, R., Carleer, R., & Buntinx, M. (2018). Recent updates on the barrier properties of ethylene vinyl alcohol copolymer (EVOH): A review. *Polymer Reviews, 58*(2), 209–246. https://doi.org/10.1080/15583724.2017.1394323

Mangaraj, S., Goswami, T. K., & Mahajan, P. V. (2009). Applications of plastic films for modified atmosphere packaging of fruits and vegetables: A review. *Food Engineering Reviews, 1*(2), 133–158. https://doi.org/10.1007/s12393-009-9007-3

Mangmee, K., & Homthawornchoo, W. (2016). Antioxidant activity and physicochemical properties of rice starch-chitosan-based films containing green tea extract. *Food and Applied Bioscience Journal, 4*(3), 126–137.

Martillanes, S., Rocha-Pimienta, J., Cabrera-Bañegil, M., Martín-Vertedor, D., & Delgado-Adámez, J. (2017). Application of phenolic compounds for food preservation: Food additive and active packaging. In *Phenolic compounds - biological activity* (pp. 39–58). InTech. https://doi.org/10.5772/66885.

Martins, I. M. G., Magina, S. P., Oliveira, L., Freire, C. S. R., Silvestre, A. J. D., Neto, C. P., & Gandini, A. (2009). New biocomposites based on thermoplastic starch and bacterial cellulose. *Composites Science and Technology, 69*(13), 2163–2168. https://doi.org/10.1016/j.compscitech.2009.05.012

Mathew, S., & Abraham, T. E. (2008). Characterisation of ferulic acid incorporated starch-chitosan blend films. *Food Hydrocolloids, 22*(5), 826–835. https://doi.org/10.1016/j.foodhyd.2007.03.012

Menzel, C. (2020). Improvement of starch films for food packaging through a three-principle approach: Antioxidants, cross-linking and reinforcement. *Carbohydrate Polymers, 250*, Article 116828. https://doi.org/10.1016/j.carbpol.2020.116828

Menzel, C., González-Martínez, C., Chiralt, A., & Vilaplana, F. (2019). Antioxidant starch films containing sunflower hull extracts. *Carbohydrate Polymers, 214*, 142–151. https://doi.org/10.1016/j.carbpol.2019.03.022

Menzel, C., González-Martínez, C., Vilaplana, F., Diretto, G., & Chiralt, A. (2020). Incorporation of natural antioxidants from rice straw into renewable starch films. *International Journal of Biological Macromolecules, 146*, 976–986. https://doi.org/10.1016/j.ijbiomac.2019.09.222

Miao, Z., Zhang, Y., & Lu, P. (2021). Novel active starch films incorporating tea polyphenols-loaded porous starch as food packaging materials. *International Journal of Biological Macromolecules, 192*, 1123–1133. https://doi.org/10.1016/j.ijbiomac.2021.09.214

Michiels, Y., van Puyvelde, P., & Sels, B. (2017). Barriers and chemistry in a bottle: Mechanisms in today's oxygen barriers for tomorrow's materials. *Applied Sciences, 7*(7), 665. https://doi.org/10.3390/app7070665

Montoya, Ú., Zuluaga, R., Castro, C., Goyanes, S., & Gañán, P. (2014). Development of composite films based on thermoplastic starch and cellulose microfibrils from Colombian agroindustrial wastes. *Journal of Thermoplastic Composite Materials, 27*(3), 413–426. https://doi.org/10.1177/0892705712461663

Montoya, Ú., Zuluaga, R., Castro, C., Vélez, L., & Gañán, P. (2019). Starch and starch/bacterial nanocellulose films as alternatives for the management of minimally processed mangoes. *Starch/Staerke, 71*(5–6), Article 1800120. https://doi.org/10.1002/star.201800120

Moon, K. M., Kwon, E. B., Lee, B., & Kim, C. Y. (2020). Recent trends in controlling the enzymatic browning of fruit and vegetable products. *Molecules, 25*(Issue 12). https://doi.org/10.3390/molecules25122754. MDPI AG.

Morais, E. S., Silva, N. H. C. S., Sintra, T. E., Santos, S. A. O., Neves, B. M., Almeida, I. F., & Freire, C. S. R. (2019). Anti-inflammatory and antioxidant nanostructured cellulose membranes loaded with phenolic-based ionic liquids for cutaneous application. *Carbohydrate Polymers, 206*, 187–197. https://doi.org/10.1016/j.carbpol.2018.10.051

Mordorintelligence. (2021). *Biopolymer packaging market - growth, trends, COVID-19 impact, and forecasts (2021 - 2026*. https://www.mordorintelligence.com/industry-reports/biopolymer-packaging-market.

Moreirinha, C., Vilela, C., Silva, N. H. C. S., Pinto, R. J. B., Almeida, A., Rocha, M. A. M., & Freire, C. S. R. (2020). Antioxidant and antimicrobial films based on brewers spent grain arabinoxylans, nanocellulose and feruloylated compounds for active packaging. *Food Hydrocolloids, 108*. https://doi.org/10.1016/j.foodhyd.2020.105836

Moustafa, H., Youssef, A. M., Darwish, N. A., & Abou-Kandil, A. I. (2019). Eco-friendly polymer composites for green packaging: Future vision and challenges. *Composites Part B: Engineering, 172*, 16–25. https://doi.org/10.1016/j.compositesb.2019.05.048

Nguyen Vu, H. P., & Lumdubwong, N. (2016). Starch behaviors and mechanical properties of starch blend films with different plasticizers. *Carbohydrate Polymers, 154*, 112–120. https://doi.org/10.1016/j.carbpol.2016.08.034

Nordin, N., Othman, S. H., Kadir Basha, R., & Abdul Rashid, S. (2018). Mechanical and thermal properties of starch films reinforced with microcellulose fibres. *Food Research, 2*(6), 555–563. https://doi.org/10.26656/fr.2017.2(6).110

Nunes, S. B., Hodel, K. V. S., Sacramento, G. da C., da Silva Melo, P., Pessoa, F. L. P., Barbosa, J. D. V., & Machado, B. A. S. (2021). Development of bacterial cellulose biocomposites combined with starch and collagen and evaluation of their properties. *Materials, 14*(2), 1–21. https://doi.org/10.3390/ma14020458

Núñez-Flores, R., Giménez, B., Fernández-Martín, F., López-Caballero, M. E., Montero, M. P., & Gómez-Guillén, M. C. (2012). Role of lignosulphonate in properties of fish gelatin films. *Food Hydrocolloids, 27*(1), 60–71. https://doi.org/10.1016/j.foodhyd.2011.08.015

Onyeaka, H., Obileke, K., Makaka, G., & Nwokolo, N. (2022). Current research and applications of starch-based biodegradable films for food packaging. *Polymers, 14*(6), 1126. https://doi.org/10.3390/polym14061126

Orts, W. J., Shey, J., Imam, S. H., Glenn, G. M., Guttman, M. E., & Revol, J. F. (2005). Application of cellulose microfibrils in polymer nanocomposites. *Journal of Polymers and the Environment, 13*(4), 301–306. https://doi.org/10.1007/s10924-005-5514-3

Osorio, M. A., Restrepo, D., Velásquez-Cock, J. A., Zuluaga, R. O., Montoya, U., Rojas, O., & Castro, C. I. (2014). Synthesis of thermoplastic starch-bacterial cellulose nanocomposites via in situ fermentation. *Journal of the Brazilian Chemical Society, 25*(9), 1607–1613. https://doi.org/10.5935/0103-5053.20140146

Othman, S. H., Majid, N. A., Tawakkal, I. S. M. A., Basha, R. K., Nordin, N., & Shapi'i, R. A. (2019). Tapioca starch films reinforced with microcrystalline cellulose for potential food packaging application. *Food Science and Technology (Brazil), 39*(3), 605–612. https://doi.org/10.1590/fst.36017

Othman, S. H., Wane, B. M., Nordin, N., Noor Hasnan, N. Z., Talib, R. A., & Karyadi, J. N. W. (2021). Physical, mechanical, and water vapor barrier properties of starch/cellulose nanofiber/thymol bionanocomposite films. *Polymers, 13*(23), 4060. https://doi.org/10.3390/polym13234060

Paiva, W. de S., Souza Neto, F. E. de, Brasil-Oliveira, L. L., Bandeira, M. G. L., Paiva, E. de S., & Batista, A. C. de L. (2021). Staphylococcus aureus: A threat to food safety. *Research, Society and Development, 10*(14), Article e372101422186. https://doi.org/10.33448/rsd-v10i14.22186

Park, C.-W., Han, S.-Y., Seo, P.-N., Youe, J., Kim, Y. S., Choi, S.-K., & Lee, S.-H. (2019). CNF in thermoplastic starch. *Bioresources, 14*(1), 1564–1578.

Pérez-Pacheco, E., Canto-Pinto, J. C., Moo-Huchin, V. M., Estrada-Mota, I. A., Estrada-León, R. J., & Chel-Guerrero, L. (2016). Thermoplastic starch (TPS)-Cellulosic fibers composites: Mechanical properties and water vapor barrier: A review. In *Composites from renewable and sustainable materials* (pp. 85–105). InTech. https://doi.org/10.5772/65397.

Porta, R., Sabbah, M., & di Pierro, P. (2022). Bio-based materials for packaging. *International Journal of Molecular Sciences, 23*(7), 3611. https://doi.org/10.3390/ijms23073611

Rachtanapun, P., & Tongdeesoontorn, W. (2009). Effect of antioxidants on properties of rice flour/cassava starch film blends plasticized with sorbitol. *Natural Science, 43*, 252–258.

Rodrigues, F. A. M., dos Santos, S. B. F., Lopes, M. M. de A., Guimarães, D. J. S., de Oliveira Silva, E., de Souza Filho, M. de S. M., & Ricardo, N. M. P. S. (2021). Antioxidant films and coatings based on starch and phenolics from Spondias purpurea L. *International Journal of Biological Macromolecules, 182*, 354–365. https://doi.org/10.1016/j.ijbiomac.2021.04.012

Rosenboom, J. G., Langer, R., & Traverso, G. (2022). Bioplastics for a circular economy. *Nature Reviews Materials, 7*(2), 117–137. https://doi.org/10.1038/s41578-021-00407-8

Santos, T. A., & Spinacé, M. A. S. (2021). Sandwich panel biocomposite of thermoplastic corn starch and bacterial cellulose. *International Journal of Biological Macromolecules, 167*, 358–368. https://doi.org/10.1016/j.ijbiomac.2020.11.156

Sepúlveda, L., Romaní, A., Aguilar, C. N., & Teixeira, J. (2018). Valorization of pineapple waste for the extraction of bioactive compounds and glycosides using autohydrolysis. *Innovative Food Science and Emerging Technologies, 47*, 38–45. https://doi.org/10.1016/j.ifset.2018.01.012

Shiku, Y., Yuca, P., And, H., & Tanaka, M. (2003). Effect of pH on the preparation of edible films based on fish myofibrillar proteins. *Fisheries Science, 69*, 1026–1032. https://doi.org/10.1046/j.0919-9268.2003.00722.x

Shrestha, L., Kulig, B., Moscetti, R., Massantini, R., Pawelzik, E., Hensel, O., & Sturm, B. (2020). Optimisation of physical and chemical treatments to control browning development and enzymatic activity on fresh-cut apple slices. *Foods, 9*(1). https://doi.org/10.3390/foods9010076

Singh, G. P., Bangar, S. P., Yang, T., Trif, M., Kumar, V., & Kumar, D. (2022). Effect on the properties of edible starch-based films by the incorporation of additives: A review, 1987 *Polymers, 14*(10). https://doi.org/10.3390/polym14101987.

Souza, V. G. L., Mello, I. P., Khalid, O., Pires, J. R. A., Rodrigues, C., Alves, M. M., & Coelhoso, I. (2022). Strategies to improve the barrier and mechanical properties of pectin films for food packaging: Comparing nanocomposites with bilayers. *Coatings, 12*(2), 108. https://doi.org/10.3390/coatings12020108

Souza, M. C., Santos, M. P., Sumere, B. R., Silva, L. C., Cunha, D. T., Martínez, J., & Rostagno, M. A. (2020). Isolation of gallic acid, caffeine and flavonols from black tea by on-line coupling of pressurized liquid extraction with an adsorbent for the production of functional bakery products. *LWT, 117*, Article 108661. https://doi.org/10.1016/j.lwt.2019.108661

Torres, F. G., Arroyo, J. J., & Troncoso, O. P. (2019). Bacterial cellulose nanocomposites: An all-nano type of material. *Materials Science and Engineering: C, 98*, 1277–1293. https://doi.org/10.1016/j.msec.2019.01.064

Trovatti, E., Serafim, L. S., Freire, C. S. R., Silvestre, A. J. D., & Neto, C. P. (2011). Gluconacetobacter sacchari: An efficient bacterial cellulose cell-factory. *Carbohydrate Polymers, 86*(3), 1417–1420. https://doi.org/10.1016/j.carbpol.2011.06.046

Vasile, C., & Baican, M. (2021). Progresses in food packaging, food quality, and safetyzcontrolled-release antioxidant and/or antimicrobial packaging. *Molecules, 26*(5), 1263. https://doi.org/10.3390/molecules26051263

Verduin, J. (2020). Photodegradation products and their analysis in food. *Food Science and Nutrition, 6*(3), 1–16. https://doi.org/10.24966/FSN-1076/100067

Vilela, C., Kurek, M., Hayouka, Z., Röcker, B., Yildirim, S., Antunes, M. D. C., & Freire, C. S. R. (2018). A concise guide to active agents for active food packaging. *Trends in Food Science and Technology, 80*, 212–222. https://doi.org/10.1016/j.tifs.2018.08.006

Wang, X. H., Cai, C., & Li, X. M. (2016). Optimal extraction of gallic acid from Suaeda glauca Bge. Leaves and enhanced efficiency by ionic liquids, 2016 *International Journal of Chemical Engineering*. , Article 5217802. https://doi.org/10.1155/2016/5217802.

Wang, X., Guo, C., Hao, W., Ullah, N., Chen, L., Li, Z., & Feng, X. (2018). Development and characterization of agar-based edible films reinforced with nano-bacterial cellulose. *International Journal of Biological Macromolecules, 118*, 722–730. https://doi.org/10.1016/j.ijbiomac.2018.06.089

Wang, D. W., Xu, Y. J., Li, X., Huang, C. M., Huang, K. S., Wang, C. K., & Yeh, J. T. (2015). Mechanical retention and waterproof properties of bacterial cellulose-reinforced thermoplastic starch biocomposites modified with sodium hexametaphosphate. *Materials, 8*(6), 3168–3194. https://doi.org/10.3390/ma8063168

Wan, Y. Z., Luo, H., He, F., Liang, H., Huang, Y., & Li, X. L. (2009). Mechanical, moisture absorption, and biodegradation behaviours of bacterial cellulose fibre-reinforced starch biocomposites. *Composites Science and Technology, 69*(7–8), 1212–1217. https://doi.org/10.1016/j.compscitech.2009.02.024

Wongprayoon, S., Tran, T., Gibert, O., Dubreucq, E., Piyachomkwan, K., & Sriroth, K. (2018). Characterization of crystalline structure and thermostability of debranched chickpea starch-lauric acid complexes prepared under different complexation conditions. In *Chiang Mai J. Sci* (Vol. 45, pp. 1–15). http://epg.science.cmu.ac.th/ejournal/.

Yildirim, S., Röcker, B., Pettersen, M. K., Nilsen-Nygaard, J., Ayhan, Z., Rutkaite, R., & Coma, V. (2018). Active packaging applications for food. *Comprehensive Reviews in Food Science and Food Safety, 17*(Issue 1), 165–199. https://doi.org/10.1111/1541-4337.12322. Blackwell Publishing Inc.

Yoon, S. do, Kim, Y. M., Kim, B. il, & Je, J. Y. (2017). Preparation and antibacterial activities of chitosan-gallic acid/polyvinyl alcohol blend film by LED-UV irradiation. *Journal of Photochemistry and Photobiology B: Biology, 176*, 145–149. https://doi.org/10.1016/j.jphotobiol.2017.09.024

Zarandona, I., Puertas, A. I., Dueñas, M. T., Guerrero, P., & de la Caba, K. (2020). Assessment of active chitosan films incorporated with gallic acid. *Food Hydrocolloids, 101*, Article 105486. https://doi.org/10.1016/j.foodhyd.2019.105486

Zhang, C., Yang, Z., Shi, J., Zou, X., Zhai, X., Huang, X., & Xiao, J. (2021). Physical properties and bioactivities of chitosan/gelatin-based films loaded with tannic acid and its application on the preservation of fresh-cut apples. *LWT, 144*. https://doi.org/10.1016/j.lwt.2021.111223

Zhao, Y., & Saldaña, M. D. A. (2019). Use of potato by-products and gallic acid for development of bioactive film packaging by subcritical water technology. *The Journal of Supercritical Fluids, 143*, 97–106. https://doi.org/10.1016/j.supflu.2018.07.025

Zhao, Y., Tagami, A., Dobele, G., Lindström, M. E., & Sevastyanova, O. (2019). The impact of lignin structural diversity on performance of cellulose nanofiber (CNF)-starch composite films. *Polymers, 11*(3), 538. https://doi.org/10.3390/polym11030538

Zhong, T., Liang, Y., Jiang, S., Yang, L., Shi, Y., Guo, S., & Zhang, C. (2017). Physical, antioxidant and antimicrobial properties of modified peanut protein isolate based films incorporating thymol. *RSC Advances, 7*(66), 41610–41618. https://doi.org/10.1039/c7ra07444a